RIVISTA
DEL
NUOVO CIMENTO
A CURA DELLA SOCIETÀ ITALIANA DI FISICA

VOL. I Ottobre - Dicembre 1969 N. 4

Equations of State at High Pressure and the Earth's Interior.

E. BOSCHI and M. CAPUTO

Istituto di Fisica e Istituto di Geodesia dell'Università - Bologna

(ricevuto il 29 Settembre 1969)

1. Introduction. 441
2. The Earth's core. 444
3. Equations of state from the Thomas Fermi model. 451
3·1. The Thomas-Fermi equation. 451
3·2. Equations of state from the Thomas-Fermi model. 454
3·3. Equations of state from the Thomas-Fermi-Dirac model. 458
3·4. Thomas-Fermi equations of state for the case of incomplete degeneracy. 460
3·5. Generalized Thomas - Fermi theory for arbitrary degeneracy. 462
4. Relation of the Thomas-Fermi equations of state to Bridgman's measurements. 465
5. Equation of state derived from the theory of finite strain. 469
6. Murnaghan's equation of state. 475
7. Equations of state derived from inter-atomic forces. 475
8. Grüneisen's equation of state. 479
9. Equation of state from Debye theory. 482
10. Equation of melting. 484
11. Compression of solids by strong shock waves. 486
12. Interpretation of shock - wave data. 492
13. Relation of Thomas-Fermi equations of state to shock-wave measurements. 495

1. – Introduction.

The present definite knowledge of the Earth's interior is supported by measurements of seismic-wave velocity, free-oscillation periods, their decay, moments of inertia and average density.

The major divisions of the internal structure are mantle and core, whose

dimensions and properties are known with remarkable precision (Fig. 1, 2). The core constitutes about one third, the mantle two thirds, of the whole mass. Both are further divided by seismologists: as any proper geological unit, the mantle is subdivided into lower, middle and upper mantle. Similarly we distinguish an inner and outer core, with a somewhat complex transition region in between. The chemical difference between mantle and core has been

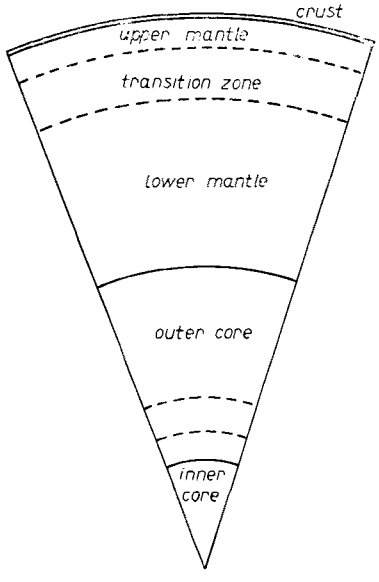

Fig. 1. – Major divisions of the Earth's interior, true scale; the crust corresponds to a 40 km continental crust.

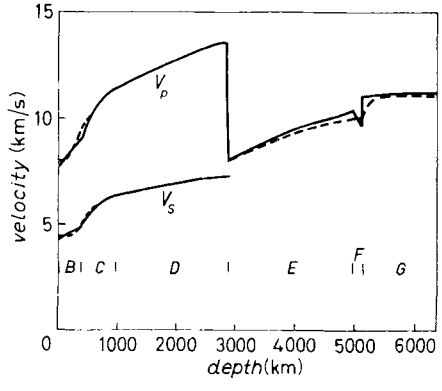

Fig. 2. – The seismic evidence for the internal structure of the Earth: velocities as a function of depth, after JEFFREYS [1] (solid curves) and GUTENBERG [2] (dashed curves).

confirmed in recent years by experiments with shock pressures equal to those of the core. However the question is by no means completely closed.

The hypothesis of an iron core *vs.* a silicate mantle depended originally upon the recognition that meteorites—iron and stony—furnished samples of an early stage of the chemical origin of inner planets. Now Fig. 3 is [3, 4] the

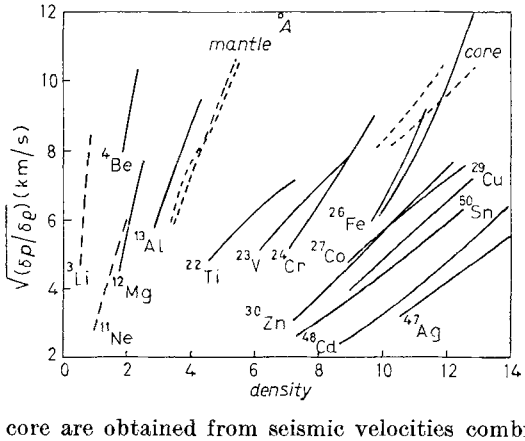

Fig. 3. – Hydrodynamical velocity, $(\partial p/\partial \varrho)^{\frac{1}{2}}$, *vs.* density. The solid curves are shock data for metals; the dashed lines are from static compressions. The dashed curves for mantle and core are obtained from seismic velocities combined with representative density distributions. The circle labeled *A* is for dunite at 2.4 megabar. (For references, see [5]).

best evidence. Here a number related to the seismic velocities (*) is plotted against density for the metals through the transition group; the solid curves are from laboratory experiments and the broken curves show the same quantities for mantle and core. From these data it is not possible to make a core of light metals or their oxygen compounds, and a mantle of heavy metals. Transformation of light compounds to a metallic state may take place in the Earth, but the density of the core demands a metal of the transition group, and only iron is sufficiently abundant. The properties of iron are close to those required and can be adjusted with small amounts of alloying elements. Figure 3 is the best demonstration that core and mantle are chemically distinct.

From another point of view, direct comparisons of pressure-density relationships of known materials with the known pressure-density variation of the Earth would allow various assumed compositions to be rejected or accepted as reasonable possibilities. Until about ten years ago, comparisons of pressure-

TABLE I. – *Some comparisons of properties of the Earth's core with measured values for iron.* (These averages are founded on data now out of date, but sufficient for our indicative purposes.)

	Depth (km)	Sound velocity (km/s)		Pressure $\cdot 10^{12}$ (*) Model B	Density (*) Model B
		JEFFREYS [1]	GUTENBERG [2]		
Earth: outer	2900	8.10	8.00	1.33	9.7
core	4980	10.44	10.04	3.22	12.0
inner	5120	9.40	10.1	3.33	15.0
core	6370	11.31		3.94	17.9
Iron (after [9])		7.85		1.22	11.03
		8.49		1.68	11.56
		9.53		2.85	12.56
		9.98		3.48	12.95
		(Iron — GUT.)/GUT.		(Iron — B)/B	(Iron — B)/B
Difference		— 2%		— 9%	+13%
		— 15%		— 50%	— 4%
		— 5%		— 16%	— 20%
				— 15%	— 25%

(*) BULLEN [8].

(*) The number related to the seismic velocities is $(K/\varrho)^{\frac{1}{2}} = (V_S^2 - \frac{4}{3} V_P^2)^{\frac{1}{2}}$, where K is the incompressibility.

density relations could be made only at the moderate pressure obtainable with static apparatus ($\leqslant 10^{11}$) (*). The recent development of the shock-wave methods for the determination of equations of state has allowed such comparisons. In fact the measurements of ALTSHULER and others [6] on iron and other metals at pressure up to $5 \cdot 10^{12}$ give comparisons at pressures as high as those at the centre of Earth ($\approx 3.5 \cdot 10^{12}$). These experimental data have been used by KNOPOFF and MACDONALD [7] to study the core composition. Their results are that the density of iron is somewhat larger ($\approx$ 10 to 20%) than the densities of the core and that a mean atomic number of about 23 is consistent with the core conditions.

TABLE II. – *Density, pressure, and incompressibility of iron.*

ϱ	$P \cdot 10^{12}$	$K \cdot 10^{12}$	K/ϱ ((km/s)^2)
7.87	0	1.68	21.4
8.35	0.111	2.12	25.5
8.83	0.245	2.61	29.7
9.32	0.402	3.17	34.2
9.83	0.586	3.81	38.9
10.35	0.798	4.52	43.8
10.87	1.039	5.31	49.0
11.39	1.312	6.18	54.4
11.93	1.617	7.14	60.0
12.48	1.962	8.21	65.9
13.03	2.342	9.37	72.1
13.61	2.765	10.64	78.5
14.18	3.232	12.03	85.1
14.78	3.742	13.53	92.0
15.34	4.298	15.16	98.8
15.93	4.916	16.91	106.1

The data of ALTSHULER and others for iron are reproduced in Table I together with some of the reported values for the core [1, 2, 8]. The correspondence between sound velocity and pressure is seen to be fairly close for the outer core although the correspondence in densities is less close. Table II reports the main characteristics of iron determined by means of the Birch-Murnaghan equation of state.

2. – The Earth's core.

The existence of a core within the Earth was suggested by WIECHERT in 1897. In 1906 OLDHAM gave a seismologic proof of the validity of Wiechert's

(*) Throughout this work, we use c.g.s. units.

hypothesis. In 1913 GUTENBERG estimated that the distance of core boundary from the Earth's surface should be about 2900 km. A recent value of such a distance, 2883 km, is that of BULLEN [10]. This value has emerged from an analysis of free-oscillation data; but further analysis of these oscillations may possibly force a modification of this result [11].

JENSEN [12] suggested the possibility of using the Thomas-Fermi model to speculate about the state of matter at the pressures which are in the Earth's core. He made an interpolation curve for iron, connecting the experimental pressure-density relation with the Thomas-Fermi curve by means of the seismic velocities in the Earth's core (see Fig. 4).

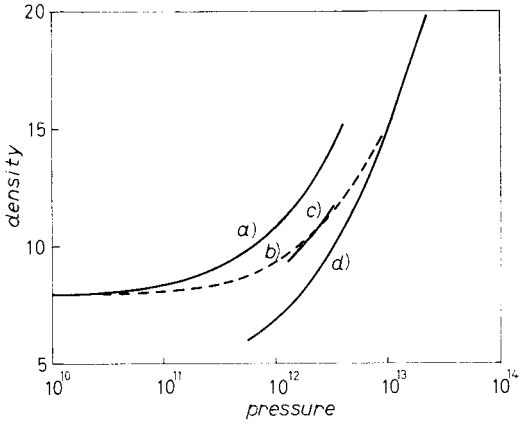

Fig. 4. – Jensen's interpolation curve for iron, connecting the experimental pressure-density relation with the Thomas-Fermi curve: *a*) Murnaghan curve for iron; *b*) Jensen's interpolation; *c*) Earth's core, after BULLEN; *d*) Thomas-Fermi curve for iron, after JENSEN.

KUHN and RITTMAN [13] have shown that, even under the most favourable conditions, the time required to separate liquid iron from silicates is much larger than the age of the Earth. That should conflict with one of the arguments supporting the hypothesis that the core is made of iron separated from silicates: the immiscibility of iron and silicates. Then they suggested a core made up of undifferentiated solar matter rich in hydrogen. However it was shown by WIGNER and HUNTINGTON [14] and by KRONIG, DE BOER and KORRINGA [15] that a significant amount of hydrogen at the core pressure would yield a material whose density is not suficiently great compared with that in the core of the Earth. In fact the calculations lead to a density for metallic hydrogen of about one at the pressure of the core, and it is clear that the hydrogen content must be limited to a smaller fraction, probably even less than the 10% by mass proposed by KRONING, DE BOER and KORRINGA (see also [16, 17]). It is evidently more reasonable to reserve hydrogen for the giant planets, which have mean densities in the neighborhood of one, than to attempt the construction, with so light elements of small planets having mean densities between 4 and 5.5.

BRIDGMAN [18-20] obtained in the laboratory static pressures of about 10^{11}; these pressures correspond to a depth of only 250 km in the Earth. Therefore large extrapolations are necessary to reproduce the conditions of the Earth's core. In many cases such extrapolations do not seem acceptable, as shall be seen in a following Section.

RAMSEY [16, 21, 22] suggested that the large increase of density at the core boundary is due to a pressure transition from the molecular to a metallic phase, rather than to the appearance of a new material such as an alloy of iron and nickel. Thus he assumes, in first approximation, that the Earth is of uniform chemical composition (below the crustal layer) which he identifies with olivine: a mixture of 90% magnesium ortho-silicate and 10% iron ortho-silicate. Originally RAMSEY put forward his hypothesis to account for the densities of the terrestrial planests. On his hypothesis the pressure at the boundary of the core will be characteristic of the chemical composition of the material which he assumes is the same for all the terrestrial planets.

A very important result is that of BULLEN [23], who found strong evidence for the inner-core solidity.

KUIPER [24] has pointed out that the dimensions and masses of the terrestrial planets show that Ramsey's hypothesis is untenable. Rabe's work [25] on the orbit of Eros and the more accurate values of the masses of Mercury and Venus rule it out on astronomical grounds.

Recent revisions [10, 16] of the estimated Mars radius make this conclusion open to question.

KUIPER [27] also observed that Kuhn and Rittman's objections used by RAMSEY to criticize the iron core, cannot, on empirical grounds, apply to planets. In fact the separation of iron and silicate phases is clearly shown in large meteorites which almost certainly derived from asteroidal bodies of roughly 500 km in diameter. Therefore at least experimental evidence of the separation of iron and silicates exists, while the opposite thesis has never been verified.

ELSASSER [28] compares the estimates of the densities and compressibilities of a larger number of elements and compounds found experimentally by BRIDGMAN, for pressures up to 10^{11}, with the limiting computed values at pressures of the order of 10^{13} and above obtained from the Thomas-Fermi model. ELSASSER interpolates in the gap between 10^{11} and 10^{13} and states that the densities of all elements can be determined as functions of the pressure in this range, with a maximum error of at most 15 to 20%. In comparing the density variation within the Earth with his interpolated curves, ELSASSER finds strong support to the theory that the mantle consists mainly of silicates and the core of iron, thus excluding the possibility of Ramsey's hypothesis. He is also able to give an atomic number to the Earth's core. This atomic number, 29, is to be compared with the atomic number of iron (26) and nickel (28). At the same time ELSASSER finds some discrepancies between his extrapolated curves and geophysical data. We shall examine more critically Elsasser's results in a following Section.

BULLEN [29] has analysed from a different point of view the problem and disagrees with Elsasser's findings. From his Earth model A, BULLEN found that there was no noticeable difference in the incompressibility gradient $\mathrm{d}K/\mathrm{d}p$

between the base of the mantle and the top of the core. Moreover there was only a 5% difference in the value of K across the core-mantle boundary. These features are in marked contrast to the large changes in the density and rigidity at the boundary. The change in K is a diminution from the mantle to the core. However, interpolating between experimental data at 10^{11} and theoretical results at 10^{13} of pressure, a slight increase of K is found in the transition from the mantle to the core. Then BULLEN [29, 30] assumed that K and $\mathrm{d}K/\mathrm{d}p$ are smoothly varying functions below a depth of 1000 km (model B). This implies that at high pressure the compressibility of a substance is independent of its chemical composition. More recent theoretical works indicate that there is some small variation of K with atomic number at high pressure, showing, however, that Bullen's hypothesis is a good approximation. BULLEN can so estimate the density at the core-mantle boundary obtaining 9.7. BULLARD [31] has investigated, by an independent method, the permissible density distributions within the Earth and has concluded that Bullen's estimate of 9.7 at the core-mantle boundary should not be in error by more than 0.5. Recent analyses of free-Earth-oscillation data have confirmed Bullen's results. Moreover on the grounds of his results, BULLEN [32] gave an important contribution analysing Elsasser's work and showing that it has some internal inconsistencies. In fact his calculations lead to the statement that the atomic number of the outer core (region E) should be almost 6 units less than that found by ELSASSER. However, if such a reduction does not overcome the six units, Elsasser's main result shall be supported, *i.e.* the region E would still be iron and nickel. But some aspects of Bullen's calculations suggest that the reduction could be greater than six units and therefore the region E may consist of a modification of ultra-basic rocks.

UREY [33] has put forward a theory for the evolution of the planets, which mainly rests on physical chemistry, concluding, on several grounds, that the Earth's core has an iron composition. BULLEN questions a number of his arguments, although agreeing that the inner core is chemically distinct from the rest of the Earth and of the outer part of the core.

BIRCH [34] reviewed the hypothesis of RAMSEY and of KRONIG, DE BOER and KORRINGA, and concluded that the core is mainly iron-nickel, although he noted that the density of the core is perhaps 10 to 20% less than that of iron or iron-nickel at core conditions. Some years later, BIRCH [35] stated an upper bound, near 13, to the Earth's central density. If this result is accepted, it entails a negative rigidity gradient in the lower core [10] and hence leads to confirmation of the inner-core solidity.

KNOPOFF and UFFEN [36] have extended the quantum-statistical calculations of the densities of the pure elements to solid compounds. Then they have interpolated between the Bridgman experimental data and their theoretical results to obtain pressure-density curves for all probable constituents. The interpo-

lation is improved by means of Birch-Murnaghan's semi-empirical theory of finite strain. As we shall see in a following Section the quantum method is strictly valid at absolute zero of temperature. KNOPOFF and UFFEN estimate, however, that providing the temperature at the core boundary does not exceed 10 000°, the errors should be less than 8%. For the temperature range $(0 \div 5300)°$ the representative atomic number (defined as the atomic number of a hypothetical pure element which has the same pressure-density relationship as the considered substance) lies between 12.5 and 13.5 with the corresponding range of composition for an olivine mantle of from 47% to 63% Mg_2SiO_4. The representative atomic number of the outer part of the core was found to be 22, intermediate between iron and silicates. Provided that there are no phase transitions, a core with an atomic number 22, composed of iron, fayalite (Fe_2SiO_4) and forsterite (Mg_2SiO_4), would have an iron content of nearly 90%. However, concluding this necessarily incomplete review of the work about the Earth's core, we can say that the core composition is not yet defined.

Perhaps the core consists of a material whose representative atomic number is close to that of iron with the addition of some substance of higher atomic number.

Meteorites and the fact that iron is *probably* liquid at the temperatures and pressures at which the silicates are probably solid give a further evidence for that composition. Moreover a ferromagnetic core should explain the origin of the Earth's magnetic field. The assumption that the relative abundances of the chemical elements in the Earth may be found from the analysis of the constitution of meteorites is somewhat supported by the probable origin of meteorites in masses of planetary dimensions and by the good agreement between the meteoritic and solar abundances for the heavy elements. The meteorites have two phases:

a) silicates, mainly olivines and pyroxenes,

b) free metals, approximately 90% of iron.

These phases occur in nearly every proportion, from stones with no free metals, to iron with no silicates.

WIECHERT suggested that the Earth possesses an iron core surrounded by a silicate mantle to explain the high mean density and central condensation. This concept is very fascinating but it is very difficult to estimate correctly the ratio between silicates and iron. The range of values of the ratio of masses of stony to iron meteorites [16, 37, 38] is very large and it seems evident that no serious quantitative argument either for or against an iron core can be drawn from such data. Moreover the variety of particles coming from space indicates that it is possible that the interior of the Earth contains a variety of components much different from those contained in meteorites.

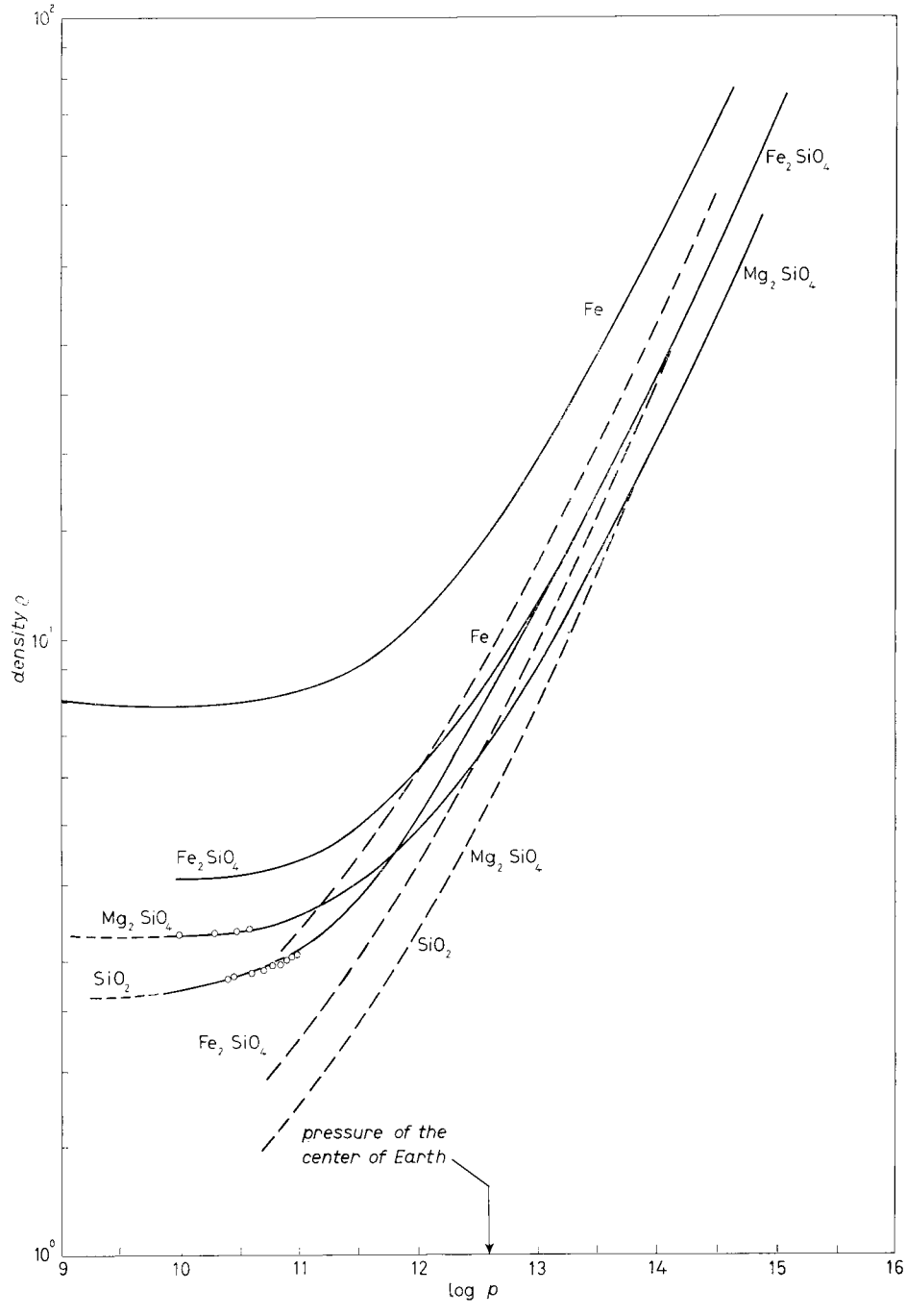

Fig. 5. – The experimental data, the Birch-Murnaghan computation and the Thomas-Fermi computations for four materials (after [36]): o experimental data; — — — Thomas-Fermi model; —— Murnaghan-Birch model.

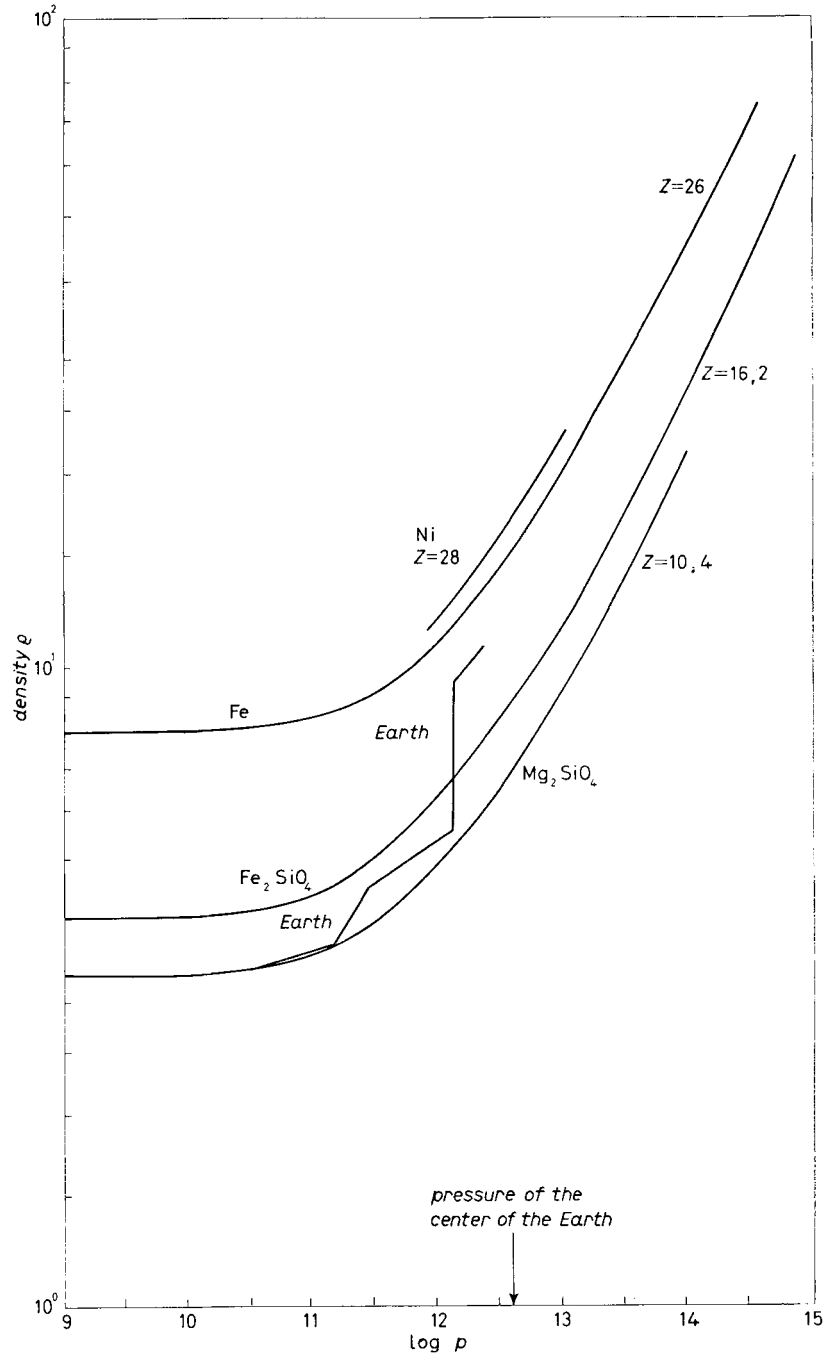

Fig. 6. – The pressure-density relation for the Earth in relation to the interpolated curves for fayalite (Fe_2SiO_4), iron and nickel at $T = 0\,^\circ K$ (after [36]).

However an inner core largely composed of nickel-iron is mainly supported by the fact that, for elements for which $Z > 28$, the abundances are very small until Z is considerably greater than 28, while curves derived through seismology do not, on reasonable assumptions, permit the representative Z for the inner core to be much greater than 28.

3. – Equations of state from the Thomas-Fermi model.

3·1. *The Thomas-Fermi equation.* – When the temperature or density is sufficiently high to introduce a large mixture of electronic quantum state, a simple statistical approximation to the equation of state can be based on independent free electrons and nuclei. In the Thomas-Fermi theory each atom of the material occupies an independent spherical cell, and the electron distribution is determined to a first approximation about a nucleus fixed in the centre of the cell. The electrons are assumed to be free Fermi-Dirac particles, and all other aspects of the quantum mechanics of atoms are ignored. Thus, the distribution of the cloud of partially degenerate nonrelativistic electrons is related to the electrostatic potential by Poisson's equation. In this manner the main effects of Coulomb interactions are included self-consistently to all orders in the electric charge.

The Thomas-Fermi equation is obtained directly from Poisson's equation by a suitable choice of variables:

$$\frac{\mathrm{d}^2\Phi}{\mathrm{d}x^2} = \frac{\Phi^{\frac{3}{2}}}{x^{\frac{1}{2}}}, \tag{1}$$

where

$$\left\{\begin{array}{l} \dfrac{Ze}{r}\Phi = V(r) - V_0, \\ r = \mu x, \\ \mu = \left(\dfrac{9\pi^2}{128Z}\right)^{\frac{1}{3}}\left(\dfrac{h}{2\pi e}\right)^2\dfrac{1}{m} = 0.885\,34\,a_0 Z^{-\frac{1}{3}}, \end{array}\right. \tag{2}$$

where Z is the atomic number, a_0 the Bohr radius for hydrogen, m the electron mass, e the electron charge, h Planck's constant, r the distance from the nucleus, V the potential and V_0 the chemical potential.

The applicable boundary conditions are that the electrostatic potential and its gradient are zero at the cell boundary r_0, and the potential has a Coulomb singularity at the origin. In dimensionless form they are

$$\Phi(0) = 1, \quad \frac{\Phi}{x} = \frac{\mathrm{d}\Phi}{\mathrm{d}x} \text{ at } x = x_0. \tag{3}$$

FEYNMAN, METROPOLIS and TELLER [39] point out that, in crystals, solutions of spherical symmetry are not strictly valid. Hence in this case (1) is not rigorously correct. More correctly, the atom should be surrounded by a polyhedron; for many cases the polyhedron may be approximated by a sphere. No strict solution of (1) is known. However $\Phi(x)$ can be developed in a semi-convergent power series:

$$\Phi = 1 + a_2 x + a_3 x^{\frac{3}{2}} + a_4 x^2 + \dots . \tag{4}$$

Once fixed a_2, the remaining coefficients can be evaluated; Table III gives the values of the first few in terms of a_2.

TABLE III. – *Coefficients of the series solution of the Thomas-Fermi equation.* a_2 is the initial slope.

$a_3 = \frac{4}{3}$	$a_8 = \frac{2}{15} a_2$
$a_4 = 0$	$a_9 = \frac{2}{27} - \frac{1}{252} a_2^3$
$a_5 = \frac{2}{5} a_2$	$a_{10} = \frac{1}{275} a_2^2$
$a_6 = \frac{1}{3}$	$a_{11} = \frac{31}{1485} a_2 + \frac{1}{1056} a_2^4$
$a_7 = \frac{3}{70} a_2^2$	

For a special value of a_2, Φ tends asymptotically to the x-axis. This solution corresponds to the free atom or, in other words, to an atom of infinite radius. The solutions obtained for values smaller than this initial slope refer to isolated atoms while larger slopes give solutions for ions [40].

Taking into account the exchange effects it is also possible to write down the Thomas-Fermi-Dirac equation (in dimensionless form):

$$\frac{\mathrm{d}^2\Phi}{\mathrm{d}x^2} = x\left[\alpha + \left(\frac{\Phi}{x}\right)^{\frac{1}{2}}\right]^3 , \tag{5}$$

where

$$\left\{\begin{array}{l} V - V_0 + a^2 = Ze^2\Phi/r , \\ r = \mu x , \\ \alpha = \frac{6^{\frac{1}{2}}}{4}(\pi Z)^{-\frac{1}{3}} = 0.211\,87 Z^{-\frac{1}{3}} . \end{array}\right. \tag{6}$$

The exchange term appears as a simple correction to the nonhomogeneous term of the differential equation. When the exchange term vanishes, eq. (5) approaches the Thomas-Fermi equation. This correction vanishes with increasing atomic number.

This simple picture of an atom has provided a most useful approximation to the equation of state of matter between the completely degenerate region at high density and low temperature and the classical ideal-gas region at high temperature and modest density. Surprisingly, the theory is also useful in many types of low-temperature, normal-density applications.

From its statistical basis, the Thomas-Fermi theory would not be expected to apply to atomic problems at normal densities and low temperatures. For instance, an interesting theorem of TELLER [41] shows that in normal conditions molecular binding cannot occur in the Thomas-Fermi approximation even when exchange corrections are made. A related problem for the theory is its well-known inability to distinguish between the ground states of the atom and the solid. However, BRILLOUIN [42] showed long ago that the Thomas-Fermi equation corresponding to zero temperature is in part a WKB approximation to Hartree theory for the atomic ground state. Actual calculations show the average electron density distribution [40] and energy eigenvalues in the atom as calculated from the electrostatic potential in Thomas-Fermi theory [43] to be in close agreement with Hartree values. Another remarkable success of the theory is its ability to predict the value of the atomic number Z at which new angular-momentum components appear in the atom [40].

An interesting development in this connection has been the demonstration of the Thomas-Fermi equation as a first step in an asymptotic expansion of the Hartree-Fock equations in powers of Planck's constant h. The next higher-order terms in this expansion were shown to include quantum corrections as well as exchange. They have been investigated by KIRZHNITS [44] and others in the Soviet Union. In their method the electron density at a point about the atom is expanded in higher commutators of the individual electron momentum operators by a standard but formal method which has in the past been used, mainly in high-temperature approximations. Only the leading term of the density expansion is used to derive the Thomas-Fermi equation, and the remaining terms represent quantum corrections which contain various local derivatives of the electrostatic potential at the point. It was pointed out that the first quantum correction term in the density correction are both of order h^2 and can be treated more consistently as perturbation corrections in the Thomas-Fermi equation rather than in the self-consistent manner used in Dirac's modification of Thomas-Fermi theory [45].

However, GROVER [46] has shown that there is a more important class of quantum corrections which were overlooked by the Kirzhnits method, and which can be similarly expanded in an asymptotic series in h. These corrections were

derived for the particle density of a bound system of particles in a one-dimensional potential by extending the Brillouin method of summing directly over individual particle states represented by WKB eigenfunctions. A more complicated asymptotic expansion in powers of h results which includes the Kirzhnits corrections but in which the leading correction term is of order h. This term has an oscillating magnitude arising from individual particle levels. In addition it is nonlocal in nature, since it depends on the spacing of the eigenvalues of the well-known WKB integral condition for bound-state eigenvalues. This is no more than a complication, since the level spacing may be consistently evaluated from the zero-order Thomas-Fermi potential. The improved density can then be used in the Poisson equation etc.

Such an iterative expansion in powers of h appears to provide, for the first time, a formal justification of the common usage of the Thomas-Fermi potential in atomic problems as a zeroth-order approximation. The success of the calculation of atomic energy levels and angular-momentum thresholds in atoms, which were mentioned previously, and the apparent accuracy of the new first-order density corrections indicate that this interaction scheme converges rapidly. Higher-order corrections will introduce great complications into the scheme, but it should at least be possible to estimate truncation errors from them.

A problem of particular interest to which this method appears well suited is the study of the manner in which the high-pressure equation of state of solids blends into the Thomas-Fermi limit at high compression. The extension of this density expansion to the spherical Hartree atom presents some analytical problems which have as yet not been completely worked out. It is clear however, that in the spherical atom the additional correction terms are of the order h^2, the same as the Kirzhnits corrections, and that there are both oscillating and slowly varying corrections of this order.

In view of the as yet incomplete theoretical picture, it is interesting to note that high-pressure experimental data already illustrate some of the expected properties of this expansion. The very regular and large periodic influence of shell structure is evident in plots of the atomic volume of the solid elements at fixed pressure [47]. All the Thomas-Fermi predictions, with and without the Kirzhnits correction as well as with the Dirac modification, parallel the average increase of atomic volumes with Z throughout the periodic table. The Kirzhnits correction is somewhat less than the amplitude of the periodic variations in all shells. It is expected that the inclusion of the oscillating correction terms mentioned above will bring the modified Thomas-Fermi theory into even better agreement with observations.

3·2. *Equations of state from the Thomas-Fermi model.* – At extremely high pressure two different procedures can be followed to determine an equation of

state (isothermal). One is to apply the classical virial theorem

$$3pv = E_{\text{pot}} + 2E_{\text{kin}} , \tag{7}$$

where p is the pressure, v is the volume per atom, E_{pot} and E_{kin} are the potential and kinetic energies, respectively. FEYNMAN, METROPOLIS and TELLER [39] have shown that the virial theorem holds in the background of the assumptions of the Thomas-Fermi model, despite the nonlinear nature of eq. (1). The latter procedure is to apply the kinetic theory of a free-electron gas. The pressure due to the bombardment of the electron gas on the boundary of the atomic sphere appears to be that due to a free-electron gas equal in density to the actual electron gas at the boundary. Such an assumption is possible since the Thomas-Fermi theory may be derived by applying free-electron relations locally. If $\varrho_e(r_0)$ is the boundary density, obtained by solution of the Thomas-Fermi equation, the pressure is then

$$p = \tfrac{2}{3} c_k \{\varrho_e(r_0)\}^{\frac{5}{3}} , \tag{8}$$

as follows from the theory of perfect gases.

We see from (8) that pressure is never zero, except when $\varrho_e(r_0) = 0$, which is only true for the isolated-atom solution corresponding to an infinite value of r_0. Introducing exchange, treating the free-electron gas by the Hartree-Fock approximation, the pressure p is now given by

$$p = \tfrac{2}{3} c_k \{\varrho_e(r_0)\}^{\frac{5}{3}} - \tfrac{1}{3} c_e \{\varrho_e(r_0)\}^{\frac{4}{3}} , \tag{9}$$

where $\varrho_e(r_0)$ is the boundary density calculated from the Thomas-Fermi-Dirac equation.

In both procedures we see that the Thomas-Fermi equation of state may be written as

$$pv = \frac{2}{15} \frac{Z^2 e^2}{\mu} x_0^{\frac{1}{2}} (\Phi(x_0))^{\frac{5}{2}} , \tag{10}$$

where $v = \frac{4}{3}\pi(\mu x_0)^3$ is the volume per atom. Numerical values over a wide range of pressures and atomic volumes are provided in Table IV and graphically represented in Fig. 7. This model gives satisfactory results for very high pressures; the lower limit of these pressures could be lowered by modifying the basic assumptions of the model on the pressure distribution within the

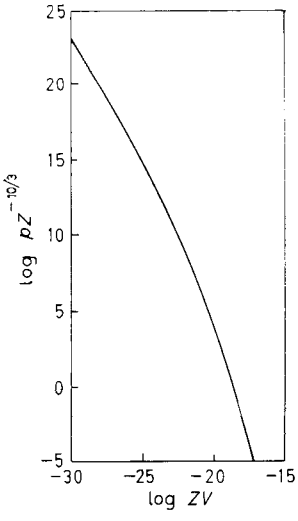

Fig. 7. – Pressure-volume relationship for the TF model (from [48]).

TABLE IV. – *Numerical solutions of the Thomas-Fermi equation over a wide range of pressures and atomic volumes (from* [48]).

Zv	$pZ^{-10/3}$	Zv	$pZ^{-10/3}$
0.70194 (−29)	0.89937 (22)	0.10149 (−21)	0.10855
0.13888 (−28)	0.28876	0.14860	0.44673 (9)
0.27965	0.89344 (21)	0.20698	0.20336
0.54172	0.29573	0.28683	0.92398 (8)
0.10969 (−27)	0.90806 (20)	0.41234	0.37791
0.21075	0.30408	0.61568	0.13803
0.42911	0.92242 (19)	0.81508	0.67383 (7)
0.83218	0.30306	0.11247 (−20)	0.29235
0.16481 (−26)	0.95881 (18)	0.15947	0.11649
0.32926	0.29796	0.22916	0.44132 (6)
0.62803	0.99752 (17)	0.31525	0.18557
0.12225 (−25)	0.32113	0.42546	0.81337 (5)
0.24388	0.98512 (16)	0.60462	0.30554
0.50482	0.28114	0.86907	0.10972
0.10167 (−24)	0.83177 (15)	0.11511 (−19)	0.49188 (4)
0.21131	0.22945	0.16982	0.16012
0.41646	0.68301 (14)	0.23018	0.65947 (3)
0.59275	0.36072	0.28384	0.35622
0.83511	0.19288	0.39324	0.13567
0.12099 (−23)	0.97270 (13)	0.62299	0.34264 (2)
0.16981	0.51634	0.89994	0.11280
0.23970	0.26897	0.13308 (−18)	0.34256 (1)
0.33954	0.13793	0.17540	0.14690
0.47549	0.71634 (12)	0.23445	0.60034 (0)
0.66784	0.36616	0.31848	0.23227
0.96257	0.17571	0.90396	0.88358 (− 2)
0.13112 (−22)	0.93451 (11)	0.16743 (−17)	0.12526
0.18736	0.44516	0.44182	0.56269 (− 4)
0.26009	0.22238	0.15196 (−16)	0.10415 (− 5)
0.35922	0.11092	0.14331 (−15)	0.68469 (− 9)
0.50818	0.51810 (10)	0.12911 (−13)	0.23937 (−15)
0.71593	0.24065		

The numbers in parentheses are the powers of ten associated with the entries.

atom. Some preliminary calculations show that for atomic numbers of the order of 30 the lower limit of validity of the new model could be of some 10^{12}.

The first work in this field was carried out by JENSEN [12], following a suggestion of SLATER and KRUTTER [49], and, some years later, by FEYNMAN, METROPOLIS and TELLER [39]. In more recent works, GILVARRY [50] and MARCH [51] have put the results into a form which should represent accurately the predictions of the Thomas-Fermi theory over the entire range of pressures. Gilvarry's procedure consists in examining the limiting forms of the equation of state at very high and very low pressures.

An approximate form is then found which is correct in these limits and which fits the available numerical data with fair accuracy in the intermediate region. The high-pressure case is very interesting for our purposes and we shall briefly consider it here. On a purely intuitive basis, with remarkable intuition, GILVARRY argues that, at sufficiently high pressures, the results, for an element with atomic number Z, must coincide with the appropriate ones for a free-electron gas, with density corresponding to Z electrons in the atomic volume v. Then the equation of state may be immediately written as

$$pv = \frac{h^2}{5m}\left(\frac{3}{8\pi}\right)^{\frac{2}{3}}\frac{Z^{\frac{5}{3}}}{v^{\frac{2}{3}}} \tag{11}$$

and this corresponds to a value of Φ, at the boundary of the atomic sphere of radius μx_0, given by

$$\Phi(x_0) = \frac{3^{\frac{2}{3}}}{x_0}. \tag{12}$$

MARCH [52] has also studied how this result follows from the properties of the dimensionless Thomas-Fermi equation, obtaining a further term in a series development of the boundary value $\Phi(x_0)$

$$\Phi(x_0) = \frac{3^{\frac{2}{3}}}{x_0}\left[1 - \frac{3^{\frac{1}{2}}}{10}x_0 + \ldots\right], \tag{13}$$

leading to the equation of state

$$pv = \frac{h^2}{5m}\left(\frac{3}{8\pi}\right)^{\frac{2}{3}}\frac{Z^{\frac{5}{3}}}{v^{\frac{2}{3}}}\left[1 - \frac{2\pi m e^2}{h^2}(4Zv)^{\frac{1}{3}} + \ldots\right]. \tag{14}$$

The first term is, of course, independent from the electronic charge; the second, involving e^2, shows the way in which the equation of state is modified at the highest pressures including the electron-nucleus and the electron-electron interactions by means of the Thomas-Fermi theory. Such an equation of state was assumed, on purely intuitive grounds, by KOTHARI [53], in his works on the mass-radius relation for the planets. At low pressures, using an asymptotic solution of the Thomas-Fermi equation, the boundary value for $\Phi(x)$ is

$$\Phi(x_0) = 296.70/x_0^3. \tag{15}$$

A fitting function for $\Phi(x_0)$, yielding the correct asymptotic forms, can be written as

$$\Phi(x_0) = \left\{\sum_{n=2}^{6} A_n x_0^{n/2}\right\}^{-1} \tag{16}$$

if the coefficients A_2, A_6 are chosen to agree with the corresponding coefficients in the asymptotic forms (12) and (15) respectively. Gilvarry's values for the remaining coefficients, chosen to obtain a good fit with the available numerical data, were slightly modified by MARCH in order that (16) should reproduce (13) for small x_0. The values of A_n thus obtained are recorded in Table V. The

TABLE V. – *Coefficients in fitted functions for* $\Phi(x_0)$ *(from* [52]).

$A_2 = 4.8075 \cdot 10^{-1}$
$A_3 = 0$
$A_4 = 6.934 \cdot 10^{-2}$
$A_5 = 9.700 \cdot 10^{-3}$
$A_6 = 3.3704 \cdot 10^{-3}$

resulting expression for $\Phi(x_0)$ then fits the existing numerical data to better than 1%. Thus a convenient Thomas-Fermi equation of state, sufficiently accurate for most purposes, is

$$p^{\frac{2}{3}}\left[\sum_{n=2}^{6} A_n \left(\frac{3v}{4\pi\mu^3}\right)^{(n+2)/6}\right] = \left(\frac{Z^2e^2}{10\pi\mu^4}\right)^{\frac{2}{3}}. \tag{17}$$

3˙3. *Equations of state from the Thomas-Fermi-Dirac model.* – Equation (9) determines the equation of state in the Thomas-Fermi-Dirac approximation. In terms of the boundary value $\Phi(r_0)$, found by solving the Thomas-Fermi-Dirac equation, we may write

$$pv = \frac{2}{15}\frac{Z^2e^2}{\mu}x_0^3\left[\left\{\frac{\Phi(x_0)}{x_0}\right\}^{\frac{1}{2}} + \alpha\right]^5\left[1 - \frac{5\alpha/4}{\{\Phi(x_0)/x_0\}^{\frac{1}{2}} + \alpha}\right]. \tag{18}$$

Figure 8 shows the graphic representation of (18) for various values of Z; no means of expressing this equation of state in a form applicable to all elements has been found.

The general form for the equation of state at the highest pressures, to the same order of accuracy as that given in eq. (14), is

$$pv = \frac{h^2}{5m}\left(\frac{3}{8\pi}\right)^{\frac{2}{3}}\frac{Z^{\frac{5}{3}}}{v^{\frac{2}{3}}}\left[1 - \frac{2\pi me^2}{h^2}(4Zv)^{\frac{1}{3}} - \frac{10\pi me^2}{3^{\frac{2}{3}}h^2}(4Zv)^{\frac{1}{3}}\alpha + \ldots\right]. \tag{19}$$

The term

$$-\frac{10\pi me^2}{3^{\frac{2}{3}}h^2}(4Zv)^{\frac{1}{3}}\alpha \tag{20}$$

which appears in (19) is simply the free-electron exchange term for Z electrons

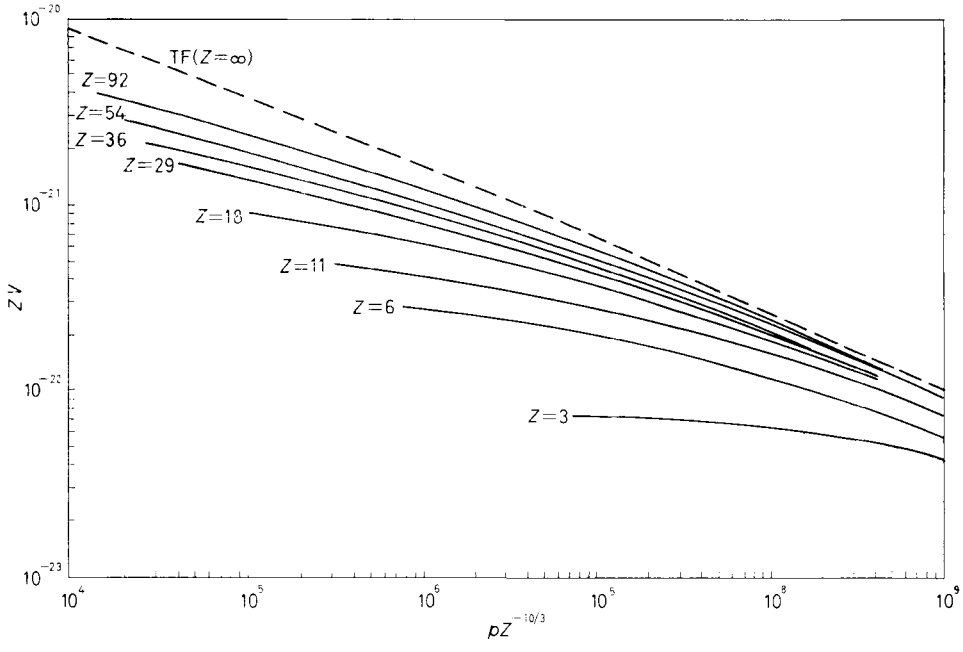

Fig. 8. – Pressure-volume relationship for the TFD model.

in a volume v. Equation (19) or the corresponding equation for the boundary value

$$\Phi(x_0) = \frac{3^{\frac{2}{3}}}{x_0}\left[1 - \frac{3^{\frac{1}{3}}}{10}x_0 - \frac{2\alpha}{3^{\frac{1}{3}}}x_0 + \ldots\right] \tag{21}$$

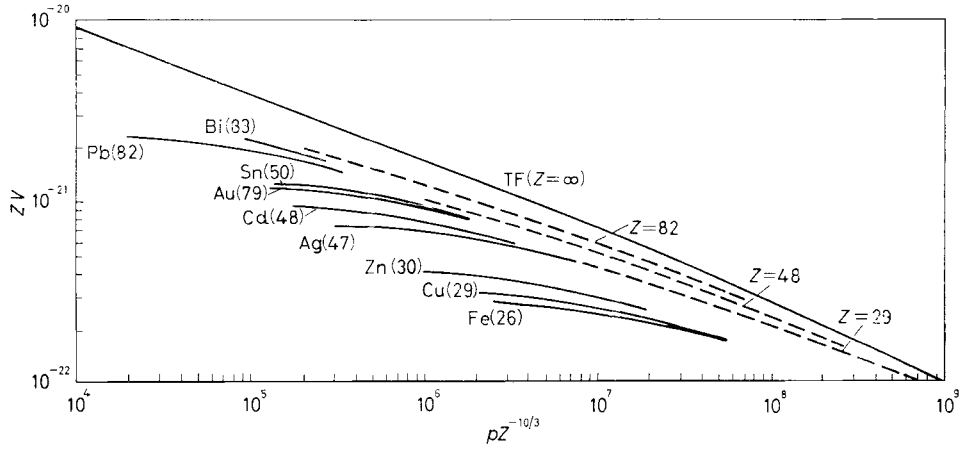

Fig. 9. – Comparison of experimental pressure-volume data reduced from ALTSHULER *et al.* with TF and TFD theoretical values for comparable atomic numbers.

should be useful in any attempt to set up analytical functions to fit the numerical data for the Thomas-Fermi-Dirac equation.

A comparison of the Thomas-Fermi-Dirac results with the experimental data of Altshuler *et al.* [6] shows that the Thomas-Fermi-Dirac equation of state is reasonably close to the experimental situation and will be accurate at a pressure not far above the range of experimental pressures (Fig. 9).

3˙4. *Thomas-Fermi equations of state for the case of incomplete degeneracy.* – Thus far it has been assumed that the electrons form a complete degenerate gas. Of course such an assumption is often not permissible. We now examine the special case of low temperature (incomplete degeneracy). In the next Subsection we shall study the general case of any temperature (arbitrary degeneracy).

GILVARRY [50] has shown that

$$p^* = p[1 + \tfrac{5}{2}(\sigma + 2\tau)\zeta(kT)^2], \tag{22}$$

where p^* is the pressure in the case of incomplete degeneracy while p is the absolute-zero value of pressure,

$$\begin{cases} \zeta = \dfrac{\pi^2\mu^2}{8Z^2e^4}, \\ \tau = \left(\dfrac{x_0}{\Phi(x_0)}\right)^2, \end{cases} \tag{23}$$

$$\sigma = \Phi^{-1}(x_0)\sum_n C_n x_0^n . \tag{24}$$

In the summation $n = 3, 4.215, 5$. Table VI gives the values of C_n.

TABLE VI. – *Coefficients C_n in equation* (24).

n	C_n
3	$-3.205\cdot10^{-1}$
4.215	$-2.331\cdot10^{-2}$
5	$-2.519\cdot10^{-3}$

The results obtained can be used whenever the temperature is low with respect to the maximum kinetic energy of the electrons near the boundary surface of the atomic sphere, namely when the inequality

$$kT \ll \frac{Ze^2}{\mu}\left(\frac{\Phi(x_0)}{x_0}\right), \tag{25}$$

holds.

GILVARRY has also given an empirical expression of the various thermodynamic functions.

The internal energy is

$$U^* = U + \frac{15}{2} pv(\sigma + 2\tau + 3\omega)\zeta(kT)^2 , \tag{26}$$

where U is the absolute-zero value. The entropy is

$$S = 15pv(\sigma + 2\tau + 3\omega)\,\zeta^2 kT . \tag{27}$$

The enthalpy is

$$H^* = H + \frac{5}{2} pv(4\sigma + 8\tau + 9\omega)\zeta(kT)^2 , \tag{28}$$

where H is the absolute-zero value.

The Helmoltz function is

$$F = U - \frac{15}{2}(\sigma + 2\tau + 3\omega)\zeta(kT)^2 . \tag{29}$$

The Gibbs function is

$$G = H - \frac{5}{2}(2\sigma + 4\tau + 9\omega)\zeta(kT)^2 . \tag{30}$$

The parameter ω, which appears in those expressions, is defined by the relation

$$\omega = x_0^{-\frac{1}{2}}\,\Phi(x_0)^{-\frac{8}{2}}\left\{\sum_m D_m x_0^{-m}\right\}^{-1} , \tag{31}$$

where $m = 0.2288,\ 0.7400,\ 2$. The values of D_m are given in Table VII.

TABLE VII. – *Coefficients D_m in equation* (31).

m	D_m
0.2288	$-5.805\cdot10^{-3}$
0.7400	$-1.925\cdot10^{-1}$
2	-3.120

KNOPOFF and MAC DONALD [7] have derived from these considerations a parameter analogous to the Grüneisen ratio

$$\gamma = \frac{1}{\varrho C_v}\left(\frac{\mathrm{d}p}{\mathrm{d}T}\right)_V , \tag{32}$$

where $(\mathrm{d}p/\mathrm{d}T)_V$ is the temperature coefficient of pressure and ϱ is the density.

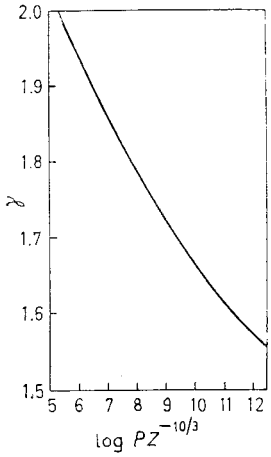

From the above expressions it is seen that to the lowest order of temperature, the Grüneisen ratio, even for the model, is independent of temperature, a conclusion inferred from the Debye model.

Figure 10 shows the numerical calculations made by KNOPOFF and MAC DONALD. The remarkable feature of this computation is that the numerical values of the Grüneisen ratio are a very slowly changing parameter over the entire range of pressures.

Fig. 10. – Pressure-Grüneisen's ratio relationship for the TF model.

3·5. *Generalized Thomas-Fermi theory for arbitrary degeneracy.* – MARCH [52] has studied the case of arbitrary degeneracy in the following manner.

Consider N free electrons enclosed in a volume v at a temperature T. The thermodynamic functions for this case are well known and may be written as follows:

kinetic or internal energy:

$$E = \frac{3}{2} NkT \left(\frac{kT}{\varepsilon_0}\right)^{\frac{3}{2}} I_{\frac{3}{2}}(\eta) , \tag{33}$$

where

$$\varepsilon_0 = \frac{h^2}{2m} \left(\frac{3N}{8\pi v}\right)^{\frac{2}{3}}$$

and η is defined by the equation

$$1 = \frac{3}{2} \left(\frac{kT}{\varepsilon_0}\right)^{\frac{3}{2}} I_{\frac{1}{2}}(\eta) ; \tag{34}$$

entropy:

$$S = \left(\frac{5}{3} \{I_{\frac{3}{2}}/I_{\frac{1}{2}}\} - \eta\right) Nk ; \tag{35}$$

free energy:

$$F = E - TS = NkT(\eta - \tfrac{2}{3}\{I_{\frac{3}{2}}/I_{\frac{1}{2}}\}) . \tag{36}$$

The I_n are integrals of the Fermi-Dirac form

$$I_n(\eta) = \int_0^\infty \frac{y^n \, dy}{1 + \exp[y - \eta]} .$$

Taking the free energy per unit volume from the free-electron theory, adding the usual electrostatic-potential energy terms and making the density ϱ a function of position, the free energy in the generalized Thomas-Fermi theory may be written

$$F=\int \varrho kT\left[\eta-\tfrac{2}{3}\{I_{\frac{3}{2}}/I_{\frac{1}{2}}\}\right]\mathrm{d}\tau-\tfrac{1}{2}e\int \varrho V_{\mathrm{e}}\,\mathrm{d}\tau-e\int \varrho V_{\mathrm{N}}\,\mathrm{d}\tau\,, \tag{37}$$

where V_{e} and V_{N} are the electrostatic potentials due to the electrons and nuclei respectively. Now we require F to be stationary with respect to variations in ϱ, subject to the normalization requirement that

$$\int n\,\mathrm{d}\tau=\text{const}\,,$$

where n is the number of electrons per unit volume. It may be seen from (34) that it is equivalent and more convenient to withe the variation of F with respect to η, so that

$$\delta F=\int \frac{\partial n}{\partial \eta}kT\eta\,\delta\eta\,\mathrm{d}\tau-e\int \frac{\partial n}{\partial \eta}V\,\delta\eta\,\mathrm{d}\tau+eV_0\int \frac{\partial n}{\partial \eta}\delta\eta\,\mathrm{d}\tau\,, \tag{38}$$

where V_0 has the meaning of a Lagrange multiplier, and

$$V=V_{\mathrm{e}}+V_{\mathrm{N}}\,.$$

The requirement

$$\delta F=0$$

gives

$$\eta=\frac{e(V-V_0)}{kT}\,. \tag{39}$$

From (34) and (39) it follows that

$$\varrho=\frac{4\pi}{h^3}(2mkT)^{\frac{3}{2}}I_{\frac{1}{2}}\left(\frac{eV}{kT}-\frac{eV_0}{kT}\right). \tag{40}$$

Combining (40) with Poisson's equation, we have the generalized Thomas-Fermi equation:

$$\nabla^2 V=\frac{16\pi^2 e}{h^3}(2mkT)^{\frac{3}{2}}I_{\frac{1}{2}}\left(\frac{eV}{kT}-\frac{eV_0}{kT}\right). \tag{41}$$

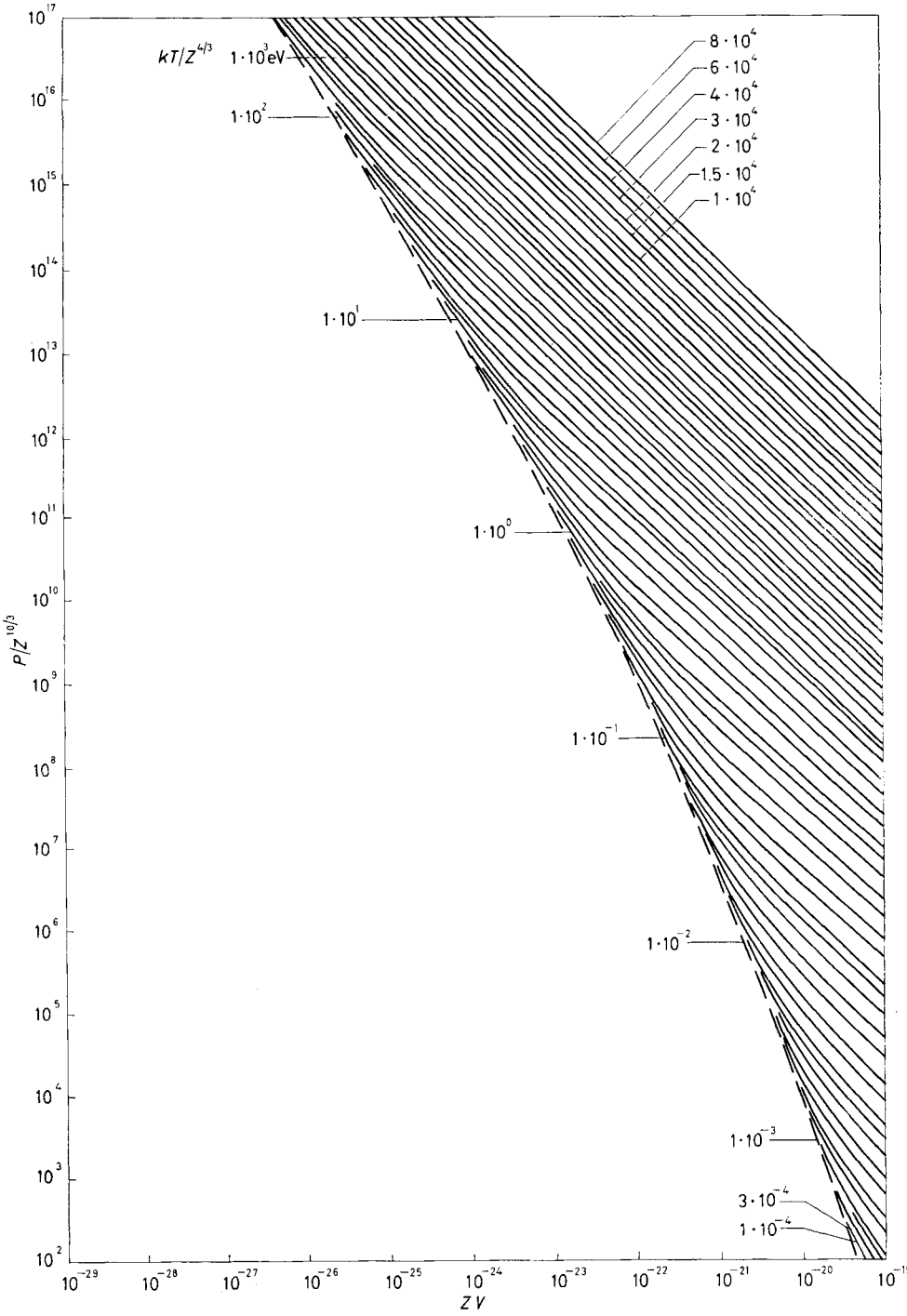

Fig. 11. – Pressure as a function of the volume for fixed temperatures (from [43]). The values of $kT/Z^{\frac{4}{3}}$ for the unlabeled curves follow the sequence shown in the upper right-hand corner.

In the sphere approximation the boundary conditions are the usual ones. In the present model the pressure may be calculated either by considering the rate of transfer of momentum between the electrons and the surface of the atomic sphere [39] or from the thermodynamic relation

$$p = -\left(\frac{\partial F}{\partial v}\right)_T . \tag{42}$$

However the result is

$$p = \frac{8\pi}{3h^3}(2mkT)^{\frac{3}{2}} kTI_{\frac{1}{2}}\left(\frac{eV(r_0)}{kT} - \frac{eV_0}{kT}\right) . \tag{43}$$

Figure 11 shows results obtained by LATTER [43]. Equation (43) is needed to study the ionization of gas mixtures in stellar interiors [54].

4. – Relation of the Thomas-Fermi equations of state to Bridgman's measurements.

By means of Bridgman's technique, it is possible to reach, in laboratory, pressures of 10^{11}. Such experimental data are represented in the left parts of Fig. 12, 13, 14. In the right part of these Figures there are the results obtained by means of the Thomas-Fermi-Dirac model at absolute zero. The Thomas-Fermi-Dirac curves are extrapolated down to pressures 10^{11} despite the fact that the model is valid only for pressures greater than 10^{13} [39]. But, taking into account that the model is more realistic for higher atomic numbers, one can think that the limit of validity increases, by a factor 10, for the light elements and decreases, by the same amount, for the heavier elements.

The theoretical curves show a steady increase of density with increasing atomic number for a given pressure. Such a correlation of density with atomic number appears fair, but not complete from Bridgman's data. On the basis of these curves ELSASSER [28] suggests that an interpolation between experimental data at low pressures and theoretical values at high pressures gives an estimate of the density in the intermediate range with an indetermination less than 20%.

But let us examine some special cases, to see the difficulties and ambiguities which are present in this procedure.

If we consider the case $Z = 92$, from Fig. 14, we find a density of 11.9 at a pressure of $0.2 \cdot 10^{12}$. Such a density is much lower than the actual uranium density for every value of pressure. From the same Figure we can see that, for uranium, it is not possible to join smoothly the experimental curve with the theoretical curve. Let us now consider copper ($Z = 29$): its density at pressure zero is 8.9, while the theoretical value at a pressure of $1.4 \cdot 10^{12}$ is only 8.4.

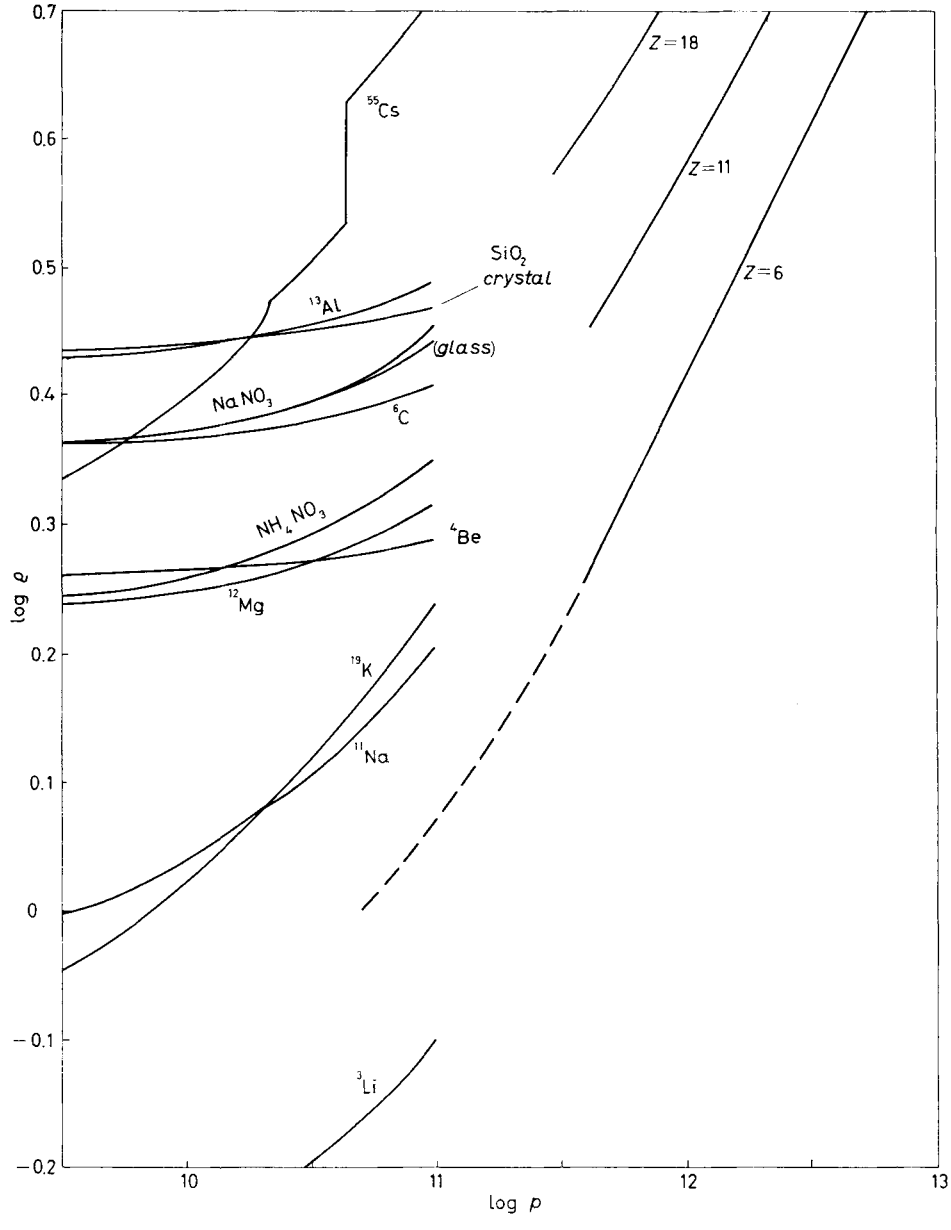

Fig. 12. – Pressure-density relationships. Curves on left-hand side: experimental results of BRIDGMAN. Curves on right-hand side: results of TFD theory. (From [28].)

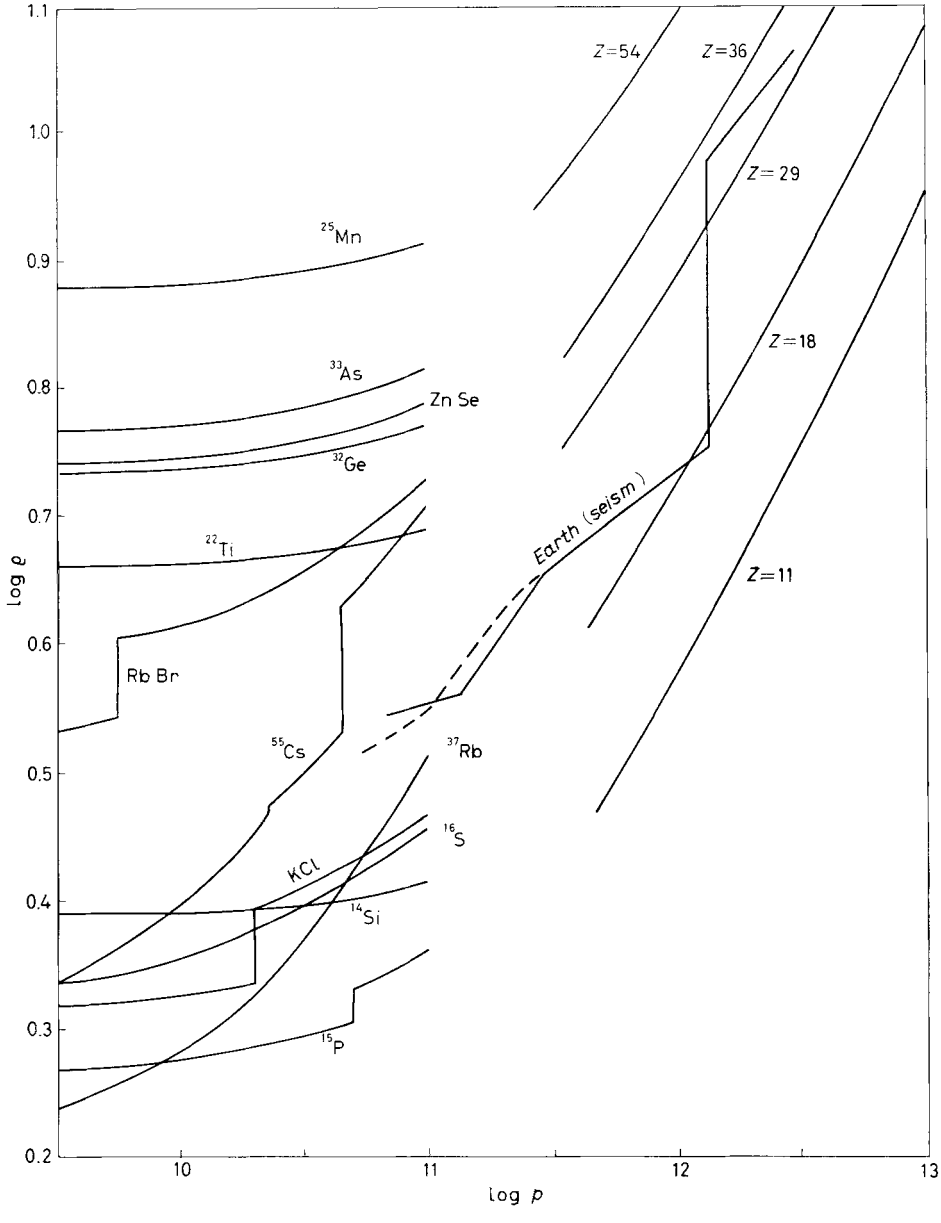

Fig. 13. – Pressure-density relationships. Curves on left-hand side: experimental results of BRIDGMAN. Curves on right-hand side: results of TFD theory. (From [28].)

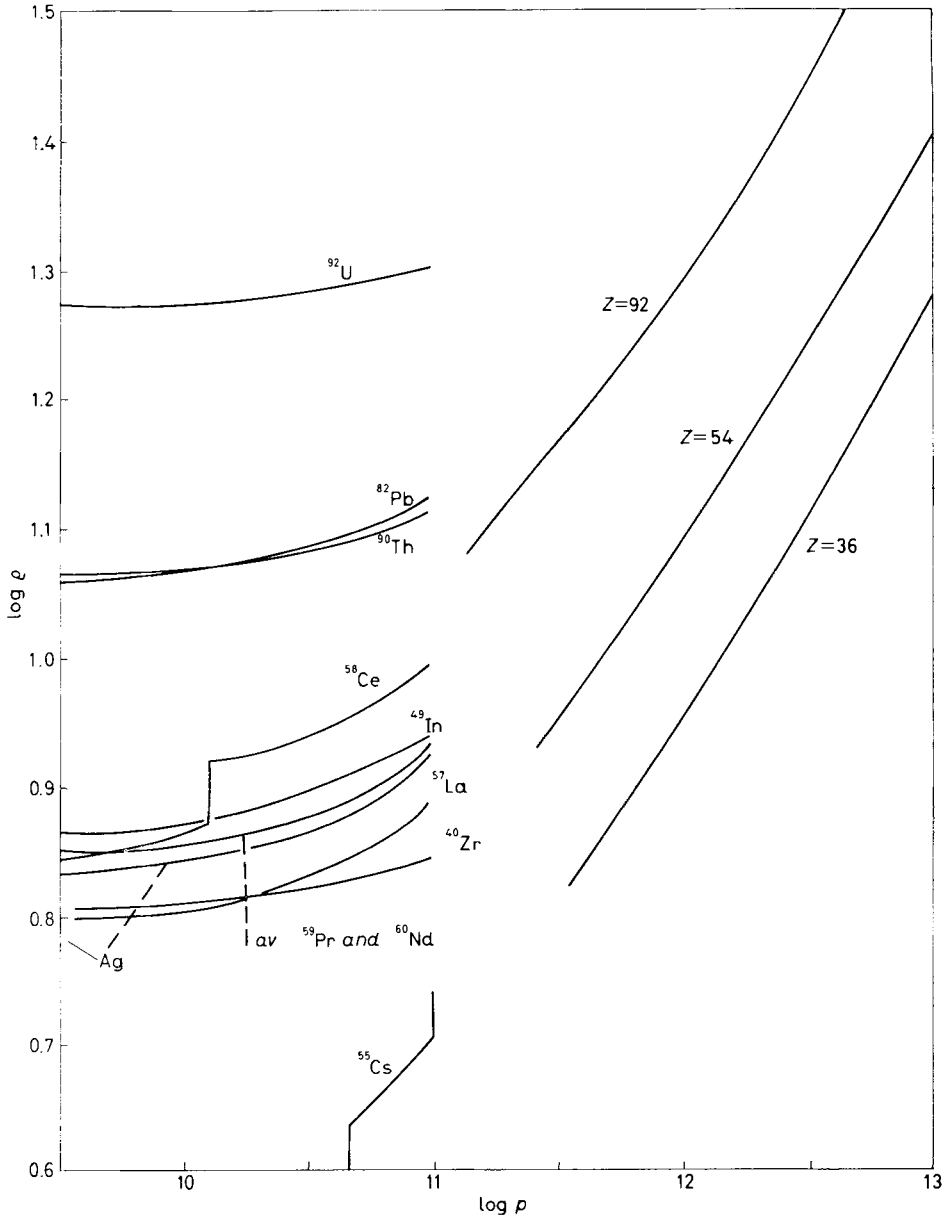

Fig. 14. – Pressure-density relationships. Curves on left-hand side: experimental results of BRIDGMAN. Curves on right-hand side: results of TFD theory. (From [28].)

Moreover the theoretical density curves of the lightest elements do not jump as the pressure increases, corresponding to the breaking-down of the inner shells. This should continue until every atom is completely broken down, the electrons then forming an imperfect degenerate Fermi gas. From this point of view the results of the Thomas-Fermi-Dirac theory, even at extremely high pressures, can at best only give an average account of what would seem to be a complicated discontinuous relation between ϱ and p for the heavier elements. Of course when the atoms are entirely broken down, the Thomas-Fermi-Dirac model is completely valid. For the heavier elements the pressures required to reach this circumstance are very high. A crude estimate by RAMSEY [22] gives for the critical pressure $\overline{p}$

$$\overline{p} \simeq Z^{\frac{5}{3}} \cdot 10^{13} .$$

For $Z \simeq 10^2$ we obtain $\overline{p} \simeq 10^{18}$. Pressures of this order and greater are found in the white dwarf stars, while, in the planets, the maximum pressure is about 10^{13} and this would seem to break completely down only the lightest elements.

5. – Equation of state derived from the theory of finite strain.

The theory of finite strain developed by MURNAGHAN [55, 56] and BIRCH [34, 57] is a rigorous development of the theory of elasticity in which no restriction is imposed on the magnitude of the strain. The theory is formally exact, but, in practice limitations arise from ignorance of the coefficients of order higher than the second which appear in the development of the strain-energy as a function of the strains. In the usual theory, only the coefficients of the second-order terms are retained in the strain-energy function; the strains are treated as small and their squares and products systematically discarded. It turns out, however, that even when only the known second-order coefficients in the strain-energy are retained, the theory of finite strain gives an excellent account of the compression of many materials, including those for which the greatest compressions have been observed: the alkali metals. It appears [57] that the third-order coefficient which occurs in the compressibility is in fact small in relation to the second-order term for a large number of materials, and, to a good approximation, may often be neglected. The complete form of the theory is required for the discussion of the effect of pressure upon individual elastic constants and velocities, but the relation between hydrostatic pressure and volume may be obtained from the thermodynamic relation

$$p = -\left(\frac{\partial F}{\partial v}\right)_T , \tag{44}$$

where F is the Helmholtz free energy and v the volume, per unit mass. In the ordinary theory of elasticity, the free energy is equated to the strain energy and expressed as a quadratic function of the strain components, higher powers being neglected. The coefficients of the second-order combinations of the strain components are the elastic constants, which depend upon the temperature. These will be termed the second-order elastic constants. Let x_i, y_i be the position vectors of a particle respectively after and before the deformation. The strain components will be referred to the strain state.

Differential relationships between adjacent particles before and after deformation are given by

$$\mathrm{d}y_i = \frac{\partial y_i}{\partial x_j}\mathrm{d}x_j \,. \tag{45}$$

The square lengths of a curve element before and after deformation are related by

$$\mathrm{d}^2 s_y = \mathrm{d}y_i \mathrm{d}y_i = \frac{\partial y_i}{\partial x_j}\mathrm{d}x_j \frac{\partial y_i}{\partial x_k}\mathrm{d}x_k \,. \tag{46}$$

In the special case

$$\mathrm{d}s_x = \mathrm{d}s_y$$

for every undeformed curve, we can rewrite

$$\frac{\partial y_i}{\partial x_j}\frac{\partial y_i}{\partial x_k} = \delta_{ik} \,. \tag{47}$$

(ε_{jk}), the strain matrix, is defined by

$$\varepsilon_{jk} = \frac{1}{2}\left(\frac{\partial y_i}{\partial x_j}\frac{\partial y_i}{\partial x_k} - \delta_{jk}\right) \,. \tag{48}$$

The element of volume after deformation, is related to that before deformation by

$$\mathrm{d}v_y = \mathrm{d}v_x \,\mathrm{Det}\left(\frac{\partial y_i}{\partial x_j}\right) \,. \tag{49}$$

Hence for the density

$$\frac{\varrho_x}{\varrho_y} = \frac{\mathrm{d}v_y}{\mathrm{d}v_x} = \mathrm{Det}\left(\frac{\partial y_i}{\partial x_j}\right) \,. \tag{50}$$

Let us consider the case of a hydrostatic strain of linear magnification α of

a medium of isotropic or cubic symmetry. Then,

$$x_i = y_i + \alpha y_i \,, \tag{51}$$

where $\alpha < 0$ means compression.

Then,

$$\frac{\partial x_i}{\partial y_i} = (1 + \alpha)\,\delta_{ij} \,, \tag{52}$$

$$\frac{\varrho_x}{\varrho_y} = (1 + \alpha)^{-3} \,, \tag{53}$$

$$\varepsilon_{jk} = \frac{1}{2}[(1 + \alpha)^{-2} - 1]\,\delta_{jk} = \varepsilon\delta_{jk} \,, \tag{54}$$

where $\varepsilon \gtreqless 0$ if $\alpha \gtreqless 0$.

Thus,

$$\frac{v_0}{v} = \frac{\varrho}{\varrho_0} = \frac{\varrho_x}{\varrho_y} = (1 + 2\varepsilon)^{\frac{3}{2}} \,, \tag{55}$$

where ε is the hydrostatic strain and the subscript zero refers to zero pressure.

To derive a pressure-density relation BIRCH [34] supposes that, for hydrostatic pressure alone, the total strain energy may be expressed in the form

$$E = \sum_{n=2}^{\infty} a_n \varepsilon^n \,,$$

where the coefficients a_n are functions only of the temperature. Then,

$$p = -\left(\frac{\partial E}{\partial \varepsilon}\right)_T \frac{\mathrm{d}\varepsilon}{\mathrm{d}v} = \frac{1}{3v_0}(1 + 2\varepsilon)^{\frac{5}{2}} \sum_{n=2}^{\infty} n a_n \varepsilon^{n-1} \,. \tag{56}$$

Introducing the isothermal incompressibility at zero pressure

$$K_0 = \frac{\mathrm{d}p}{\mathrm{d}(v_0/v)} = \frac{2}{9}\frac{a_2}{v_0} \tag{57}$$

and taking into account also (55), we obtain

$$p = \frac{3}{2} K_0 (\varrho/\varrho_0)^{\frac{5}{3}} \sum_{n=0}^{\infty} \frac{(n+2)\,a_{n+2}}{2a_2} \{(\varrho/\varrho_0)^{\frac{2}{3}} - 1\}^{n+1} \,, \tag{58}$$

or

$$p = \tfrac{3}{2} K_0 [(\varrho/\varrho_0)^{\frac{7}{3}} - (\varrho_0/\varrho_0)^{\frac{5}{3}}] \{1 + \xi[(\varrho/\varrho_0)^{\frac{2}{3}} - 1] + \ldots\} \,,$$

where

$$\xi = \frac{3a_3}{2a_2};$$

K_0 and ξ are functions of the temperature only. The convergence of the series depends on the amount of compression ε, or ϱ/ϱ_0 and on the magnitude of the coefficients of higher powers of ε. In the Earth, ε does not exceed about 0.3; which corresponds to $\varrho/\varrho_0 \approx 2$; in the mantle it is less than 0.13.

ξ is related to experimental quantities by [34]

$$\xi = -\tfrac{3}{4}[K_0' - 4],$$

where

$$K_0' = \left(\frac{\partial K}{\partial p}\right)_T \qquad \text{as} \qquad p \to 0 .$$

BIRCH [34] plotted the experimental values of $p(K_0, \varrho/\varrho_0)$ from the above formula and found that, for alkali metals at least, which themselves have large compressibilities, the data to 10^{11} of pressure correspond very closely to a value of the second-order coefficient

$$3a_3 \ll 2a_2 \qquad (\text{or } \xi \ll 1)$$

and in fact this is so for a number of other materials. Hence the theory of finite strain leads to the semi-empirical expression

$$p = \tfrac{3}{2} K_0[(\varrho/\varrho_0)^{\frac{7}{3}} - (\varrho/\varrho_0)^{\frac{5}{3}}] . \tag{59}$$

Equation (59) is obtained expressing the free energy as a single parabolic potential-energy term. If higher-order terms in the potential energy are retained, the equation of state becomes

$$p = \frac{3}{2} K_0(\varrho/\varrho_0)^{\frac{5}{3}} \sum_{n=1}^{\infty} \frac{c_n}{c_1}[(\varrho/\varrho_0)^{\frac{2}{3}} - 1]^n . \tag{60}$$

Strain here is not defined in terms of the change in dimension of an element of length as in the case of infinitesimal strain but in terms of the relative expansion or contraction of an element of area. Thus the strain tensor ε_{ij} is defined by

$$\varepsilon_{ij} = \frac{1}{2}\left\{\frac{\partial u_i}{\partial x_j} + \frac{\partial u_j}{\partial x_i} + \frac{\partial u_k}{\partial x_i}\frac{\partial u_k}{\partial x_j}\right\},$$

where

$$u_i = x_i - y_i .$$

The quadratic strain reduces to the linear strain

$$\tfrac{1}{2}(u_{i,j} + u_{j,i})$$

for small strains.

KNOPOFF [58] remarks that the construction of a quadratic strain is by no means unique. Therefore it is possible to define other quantities which are also tensors of rank two and which reduce to the proper relationship for small strains. The tensor functional

$$\eta_{ij} = f(\varepsilon_{ij}) ,$$

where

$$\frac{\mathrm{d}f(x)}{\mathrm{d}x} = 1 \qquad \text{at} \qquad x = 0 ,$$

satisfies this condition. As an example of this functional KNOPOFF considers the expansion

$$\eta_{ij} = \varepsilon_{ij} + a_2 \varepsilon_{ik}\varepsilon_{kj} + a_3 \varepsilon_{ik}\varepsilon_{kl}\varepsilon_{lj} + \dots ,$$

where ε_{ij} is the quadratic strain tensor given above.

In this case, for hydrostatic strain, the new strain tensor has diagonal components

$$\eta = -\alpha + (\tfrac{3}{2} + \alpha_2)\alpha^2 + (-a_3 - 3a_2 - 2)\alpha^3 + \dots ,$$

where α is the linear strain as before. If the series is truncated then we can invert the relationship to solve for $\alpha(\eta)$ with an approximate expression of the type

$$1 + \alpha = \left(1 - \sum_{n=1}^{m-2} c_n \eta^n\right)^b ,$$

where c_n and b are to be determined as functions of the a_n. Since the strain energy is written as a function of the invariants of the strain, a strain energy written as a function of η is sufficient and an equation of state can be obtained as before. As an example consider the case

$$\eta = -\alpha + (\tfrac{3}{2} + a_2)\alpha^2 .$$

This can be inverted to yield

$$(1 + \alpha) = [1 + (2 + 2a_2)\eta]^{-1/(2+2a_2)}$$

and the volume change is given by (53), which is rather different from the value which one would obtain by discarding the square of the strain.

Assuming, further, a single-term energy function

$$E = b\eta^2 ,$$

as before, the equation of state thus derived is

$$p = \frac{3}{2 + 2a_2} K_0\{[(\varrho/\varrho_0)^{(7+4a_2)/3} - (\varrho/\varrho_0)^{(5+2a_2)/3}] + \ldots\} , \tag{61}$$

which reduces to the Birch equation of state if $a_2 = 0$. Evidently the derivation of an equation of state based on the theory of finite strain can be criticized [58] on several grounds. Since the equations of state so derived depend upon the existence of the quadratic terms in the definition of the strain tensor, the strains must be unambiguously defined so that the quadratic, and perhaps higher-order terms, are unique. Since tensor-invariant functions of the displacement can be written which have ambiguous quadratic and higher-order terms in the linear magnification, and yet reduce to the appropriate behaviour at infinitesimal strains, an appropriate theory of finite strain must await a definition of the strain itself. Since the free energy may depend significantly upon the existence of terms of order higher than those which are quadratic in the strain, the pressure in the equation of state may be expanded in a series of ascending powers of ϱ/ϱ_0. If $m = 2$ the expansion is in powers of $(\varrho/\varrho_0)^{\frac{2}{3}} - 1$; if $m = 3$ it is in powers of $(\varrho/\varrho_0)^{(2+2a_2)/3} - 1$. The validity of the use of quadratic expressions can be shown by direct experimental measurements. The equation of state derived on the basis of the theory of finite strain becomes akin to that of an interpolation formula; extrapolation to values of ϱ/ϱ_0 significantly higher than those in the range of laboratory compressibility measurements is questionable because of the problem of the influence of higher powers of ϱ/ϱ_0.

Over small ranges of compression it may be that it is not directly possible to distinguish between two models of the equation of state.

Consider for example the two models

$$p = \tfrac{3}{2} K_0\{(\varrho/\varrho_0)^{\frac{7}{3}} - (\varrho/\varrho_0)^{\frac{5}{3}}\}\{1 + \xi[(\varrho/\varrho_0)^{\frac{2}{3}} - 1]\} , \tag{62}$$

$$p = \frac{3}{2 + 2a_2} K_0\{(\varrho/\varrho_0)^{(7+4a_2)/3} - (\varrho/\varrho_0)^{(5+2a_2)/3}\} . \tag{63}$$

Given a measurement of K_0 at $p = 0$ and a value of p at some high value of ϱ/ϱ_0, then, because of a limited range of compressibilities in the laboratory the two expressions may be equal within the limits of experimental accuracy

for a certain choice of ξ and a_2 to fit the slope and go through the required point. What is required here are very accurate experimental data on compressibility and, in addition, experimental data extending to large compressibilities.

6. – Murnaghan's equation of state.

MURNAGHAN [59], by means of the assumption that the isothermal bulk modulus

$$K = \varrho \left(\frac{\partial p}{\partial \varrho}\right)_T$$

satisfies the relation

$$K(p, T) = K_0(T) + K_0'(T)p \,, \tag{64}$$

where $K_0'(T) = (\partial K/\partial p)_T$ as $p \to 0$, obtained the following equation of state:

$$p(\varrho, T) = \frac{K_0(T)}{K_0'(T)} \{(\varrho/\varrho_0)^{K_0'(T)} - 1\} \,. \tag{65}$$

Equation (65) is, experimentally, nearly indistinguishable from the Birch-Murnaghan equation over a considerable range of compression. This fact may be understood on the basis of the uniqueness of the Taylor expansion [60].

7. – Equations of state derived from inter-atomic forces.

The inter-atomic forces can be divided into two main groups: forces of attraction and forces of repulsion. Moreover the forces of attraction can be divided into three types:

a) Coulomb forces,

b) Van der Waals forces,

c) exchange forces.

a) *Coulomb forces.* The potential energy Ψ_{Coul} for two charges, at a distance r, is given by

$$\Psi_{\text{Coul}} = -\frac{e_1 e_2}{r} \,.$$

If one or both charges are replaced by dipoles or higher multipoles, the potential

energy can be derived from this basic equation, resulting in a term proportional to $r^{-m}(m = \text{integer})$.

b) *Van der Waals forces.* The Van der Waals energy between two particles is proportional to r^{-6}. There are three mechanisms which give rise to Van der Waals energy, distinguished as « dispersion effect », « induction effect » and « orientation effect ».

The moving electrons in the first atom induce rapidly changing dipole moments in the second atom; these are proportional to the polarizability α. The mutually disturbed electrons could attract each other on the average with a potential energy:

$$\Psi_{\text{disp}} = -\frac{3}{4}\frac{\alpha^2 E_0}{r^6},$$

where E_0 is an energy value characteristic of the atom under consideration, lying between the lowest excitation energy and the ionization energy.

If one of the atoms carries a permanent dipole moment p, this will induce another dipole in the second atom proportional to αp. Primary and secondary dipoles will exert on one another forces which may be repulsive or attractive,

$$\Psi_{\text{induct}} = -2\frac{p^2\alpha}{r^6},$$

but averaged over all mutual orientations they will be attractive.

Thirdly, two permanent dipoles will also exert forces, which again, when averaged over all possible orientations, will be attractive:

$$\Psi_{\text{orient}} = -\frac{2p^4}{3kTr^6}.$$

In most cases the dispersion effect is the greatest of the three, but for very high permanent dipole moments the orientation effect may predominate. The induction effect is never the most important [44].

c) *Exchange forces.* – Exchange energy, of which homopolar chemical binding by valency forces is an example, is a typical quantum effect. Sometimes the energy is positive (repulsive) for all distances; in other cases a minimum energy occurs at small distances.

As a rule valency forces work only at very small distances. Since binding energy is due to a pair of valency electrons originating from the participating atoms, valency forces show saturation, if valency electrons are not available.

Besides the forces of attraction there must also be forces of repulsion, so that atoms (ions) attain equilibrium positions at a distance apart. This is

accomplished by the mutual repulsion of electron clouds as soon as atoms try to inter-penetrate. The numerical calculation of these forces is extremely complicated and should take place on a quantum-mechanical basis. The results [62-64], cannot as a rule be expressed by simple formulae, dependence on the distance being neither a power nor an exponential function.

The inter-atomic forces active within metals present a rather difficult problem. To account for good electrical conductivity it is assumed that electrons can move more or less freely throughout the whole volume, thus passing from one atom to its neighbours. Such free exchange of electrons makes it necessary to apply Pauli's rule. It follows that many electrons must possess a high kinetic energy. In general this excess energy is called Fermi energy; since it is positive it has to be added to the other repulsive potentials.

The cohesion may be due to the forces of attraction between the positive ions and the negative electrons.

The hypothesis that migrating electrons temporarily help to form a chemical bond between two metal atoms, these bounds continuously shifting from one neighbour to another, might also be made [65, 66].

In reality the metal does not correspond to either of the preceding hypotheses but its behaviour is somewhere in between the two. Theoretical calculations are made as approximations from either side. The homopolar bond theory will give good results for those metals which behave more or less as amphoteric elements, *i.e.* germanium, tin and bismuth. The free-electron theory [67-72] will give the best results in those cases where the electrons are only loosely bound, as in the case of the alkali metals [73].

Since energy calculations start from free ions and free electrons, a correction for ionization energy must be made in order to determine the cohesive energy. The agreement between the calculated and the observed values is most satisfactory considering that the theoretical end result is obtained as a difference between two large numbers, both of which are liable to error.

The large negative term in the energy equation is mainly due to Coulomb forces and varies theoretically as $1/r$. The repulsive Fermi energy varies theoretically as $1/r^2$.

In the case of potassium, if the calculations are made on the same basis as those for lithium and sodium, the agreement is far worse.

GOMBÀS [70], starting from somewhat different assumptions, was able to account quantitatively for the cohesive energy of potassium. Although his calculations are to be handled with some care, they give the impression that the underlying physical mechanism is right and that only the mathematical difficulties are so great as to make good agreement impossible in all cases. The theory is well enough founded to make it possible to predict that metallic hydrogen cannot exist, since the lattice energy of molecular hydrogen is far more negative than that of ionic hydrogen.

Following the suggestion of MIE [74] we may represent the mutual potential energy of two atoms or ions by the binomial expression

$$\Psi(r) = -\frac{a}{r^m} + \frac{b}{r^n}, \tag{66}$$

where the first term refers to the attractive forces, the second to the repulsive forces; m and n are constants, n being greater than m.

This expression is not, of course, more than a rough approximation; both attractive and repulsive energies may be far more complicated functions of the mutual distance r, and the saturation and orientation character of valency energy is not expressed by Mie's equation. We can see that m will have the value 1 for ionic lattices (Coulomb energy) and we may tentatively equate it to 1 for alkaline metals; it will be 6 for molecular lattices (Van der Waals energy).

Not much can be predicted theoretically about the value of n. Rough theoretical estimations put it at about 9 for ionic lattices and about 2 for alkali metal lattices (Fermi energy). It can, however, be determined experimentally from the bulk modulus [75]. Assuming that

$$p = -\left(\frac{\partial \Psi}{\partial v}\right)_T,$$

we obtain the following equation of state:

$$p = \frac{3K_0}{n-m}\left[(\varrho/\varrho_0)^{n/3+1} - \frac{a}{b}(\varrho/\varrho_0)^{m/3+1}\right]. \tag{67}$$

Using the potential function

$$\frac{A}{r^3} + \frac{B}{r^2} - \frac{C}{r},$$

derived on somewhat different grounds, BARDEEN [71] obtains

$$p = (\varrho/\varrho_0)^{\frac{4}{3}}[(\varrho/\varrho_0)^{\frac{2}{3}} - 1]\{\tfrac{3}{2}K_0 + D[(\varrho/\varrho_0)^{\frac{2}{3}} - 1]\}, \tag{68}$$

where D is a constant to be determined empirically. However it has been noted that all these relations have the limitation that they cannot be extended across polymorphic transitions. This is true also for the theory of finite strain. Moreover, the potential functions used are an unsatisfactory description of the actual inter-atomic potentials if extended over a wide range of pressures.

8. – Grüneisen's equation of state.

It is assumed that the thermal energy of a metal crystal is described adequately as the sum of the energies of a set of simple harmonic oscillators (the normal modes of the dynamical system) whose frequencies ν_α are functions only of the volume. The total mean internal energy E of the crystal (according to the statistics of quantum theory and neglecting electronic contributions) is given by (*e.g.* see [76])

$$E = \varphi(v) + \sum_{\alpha=1}^{3N} \frac{h\nu_\alpha}{\exp[h\nu_\alpha/kT] - 1} . \tag{69}$$

$\varphi(v)$ is the potential energy of the crystal with the atoms at rest in their equilibrium positions, the summation is over the $3N$ normal modes of the crystal, N being the total number of atoms and v the specific volume. The Helmholtz free energy for such a system is given by

$$A = \varphi(v) + kT \sum_{\alpha=1}^{3N} \ln\left(1 - \exp\left[-\frac{h\nu_\alpha}{kT}\right]\right) . \tag{70}$$

The external pressure is then

$$p = -\left(\frac{\partial A}{\partial v}\right)_T = -\frac{\mathrm{d}\varphi}{\mathrm{d}v} + \frac{1}{v}\sum_{\alpha=1}^{3N} \gamma_\alpha \frac{h\nu_\alpha}{\exp[h\nu_\alpha/kT] - 1} , \tag{71}$$

where γ_α is the dimensionless variable

$$\gamma_\alpha \equiv -\frac{\mathrm{d}\ln\nu_\alpha}{\mathrm{d}\ln v} , \tag{72}$$

called Grüneisen ratio for an individual oscillator.

We assume, as did GRÜNEISEN [77], that the ν_α are independent of the temperature but are density-dependent and further that all the γ_α are equal to each other, *i.e.* that the frequencies of all normal modes change proportionally to the volume in the same manner. SLATER [76] points out that this implies a relationship $\nu_\alpha = c_\alpha v^{-\gamma}$.

By such an assumption eq. (71) reduces to the Grüneisen equation of state

$$p = -\frac{\mathrm{d}\varphi}{\mathrm{d}v} + \frac{\gamma}{v} E_{\mathrm{vib}} , \tag{73}$$

where E_{vib} is the vibrational contribution to the internal energy

$$E_{vib} = \sum_{\alpha=1}^{3N} \frac{h\nu_\alpha}{\exp[h\nu_\alpha/kT]-1} .$$

For later use it is convenient to write this equation of state in one of the following forms:

$$p - p_k = \frac{\gamma}{v}(E - E_k) , \tag{74}$$

or

$$p - p_H = \frac{\gamma}{v}(E - E_H) , \tag{75}$$

where p_k and E_k are the pressure and internal energy as functions of volume at 0 °K, and p_H and E_H are the pressure and internal energy along the Hugoniot curve considered as a function of the volume only. Grüneisen's ratio γ can be expressed in terms of other thermodynamic quantities by differentiating eq. (74) with respect to E at constant v. Since γ is a function only of volume, one obtains

$$\gamma = v\left(\frac{\partial p}{\partial E}\right)_v \equiv \frac{v}{C_v}\left(\frac{\partial p}{\partial T}\right)_v \equiv -\frac{v}{C_v}\left(\frac{\partial p}{\partial v}\right)_v\left(\frac{\partial v}{\partial T}\right)_p \equiv -\frac{v}{C_p}\left(\frac{\partial p}{\partial v}\right)_S\left(\frac{\partial v}{\partial T}\right)_p , \tag{76}$$

so that at zero pressure γ can be evaluated from experimental data for the bulk modulus, thermal expansion and specific heat. The equation of state (74) was derived by assuming that all the logarithmic derivatives of the eigenfrequencies are equal. It will be noted that this assumption is not necessary for high temperatures for in the classical limit the energy of each oscillator approches KT, and the eq. (71) reduces to

$$p - p_k = \frac{3NRT}{v}\left[\frac{1}{3N}\sum_{\alpha=1}^{3N}\gamma_\alpha\right] . \tag{77}$$

This equation is identical to (74) except for the different result for Grüneisen's ratio, which now is an average value of the logarithmic derivatives. The approximation is a valid one for nearly all metals at room temperature and above, since in these cases specific-heat measurements indicate that the classical limit has been attained.

Let α be the volume coefficient of thermal expansion. Then,

$$\alpha = \frac{1}{v}\left(\frac{\mathrm{d}v}{\mathrm{d}T}\right)_p = \frac{1}{K}\left(\frac{\mathrm{d}p}{\mathrm{d}T}\right)_v ,$$

where K is the bulk modulus:

$$K = -v\frac{\mathrm{d}p}{\mathrm{d}v}\,.$$

From the expression above and (76)

$$\gamma = \frac{vK\alpha}{C_v}\,.$$

This expression, called Grüneisen's relation [75] has a number of properties that can be investigated from experimental data. γ appears to be substantially independent of the temperature and is indeed volume-dependent. The volume dependence was first determined by SLATER [76], who obtained the expression

$$\gamma = -\frac{v}{2}\frac{\partial^2 p/\partial v^2}{\partial p/\partial v} - \frac{2}{3} \tag{78}$$

for an isotropic elastic continuum with constant Poisson's ratio.

The result follows from the usual relations:

$$C_l = \sqrt{vC_{11}}\,, \tag{79}$$

$$C_t = \sqrt{\frac{(C_{11}-C_{12})v}{2}}\,, \tag{80}$$

$$K = -v\frac{\mathrm{d}p}{\mathrm{d}v} \equiv \frac{C_{11}+2C_{12}}{3}\,, \tag{81}$$

where C_l and C_t are the longitudinal and transverse wave velocities, K is the bulk modulus and C_{11}, C_{12} are the two first-order elastic constants of the isotropic medium. For constant Poisson's ratio (C_{11}/C_{12}), the relation

$$\nu_i = c/\lambda_i\,,$$

where λ_i varies as $v^{\frac{1}{3}}$, then leads (from (79) and (80) for the sound velocity) to

$$\gamma_i = -\frac{\mathrm{d}\ln\nu_i}{\mathrm{d}\ln v}\,,$$

which are equal for all modes of vibration. In particular, for a longitudinal mode,

$$\gamma = -\frac{1}{2}\frac{\mathrm{d}\ln C_{11}}{\mathrm{d}\ln v} - \frac{1}{6}\,. \tag{82}$$

Equation (81), for constant Poisson's ratio, may be rewritten

$$v\frac{\mathrm{d}p}{\mathrm{d}v} = (\text{const})\cdot C_{11}\,. \tag{83}$$

Eliminating C_{11} from (82), by means of (83), then yields the Slater's formula (78).

GILVARRY [78] showed that the expression also follows from Murnaghan's theory of finite strain, which is also based on the two assumptions mentioned above.

Both SLATER [76, 79] and GILVARRY [78], using values of first and second derivatives at zero pressure obtained from Brigdman's compressibility data, have made extensive comparisons of the γ calculated from (78) and the values obtained from the thermodynamic definition (eq. (76) above).

DUGDALE and MAC DONALD [80] modified the Slater relation to

$$\gamma = -\frac{v}{2}\frac{\partial(^2pv^{\frac{1}{3}})/\partial v^2}{\partial(pv^{\frac{1}{3}})/\partial v} - \frac{1}{3}\,, \tag{84}$$

assuming that the thermal expansion is zero in the case of Hooke's law interatomic forces. This assumption was later proved erroneous by GILVARRY [78] and BARRON [81, 82]. However (84) is in excellent agreement with zero-pressure tests.

In a recent paper KNOPOFF and SHAPIRO [83] have compared the various methods of computing Grüneisen's parameter. They have also attempted to bring them into closer agreement by taking into account the elastic moduli, the crystalline anisotropy, the effects of melting and of fluidity.

9. – Equation of state from Debye theory.

The thermal energy of a crystal is

$$U = \sum_{i=1}^{3N} \frac{h\nu_i}{\exp[h\nu_i/kT]-1}\,. \tag{85}$$

DEBYE [84] assumed that all frequencies of vibration are bounded by some maximum value ν_m, *i.e.*

$$\nu_i < \nu_m \quad \text{for all } i\,,$$

and replaced in (85) the sum by an integral:

$$U_{\mathrm{D}} = \int_0^{\nu_m} \frac{h\nu f(\nu)\,\mathrm{d}\nu}{\exp[h\nu/kT]-1}\,, \tag{86}$$

where $f(\nu)$ is the number of frequencies between ν and $\nu + \mathrm{d}\nu$. In an elastic solid

$$f(\nu) = \frac{9\nu^2}{\nu_m^3} N_0 ,$$

where N_0 is the number of atoms per unit volume. The thermal energy is then

$$U_D = \frac{9N_0}{\nu_m^3} \int_0^{\nu_m} \frac{h\nu^3 \mathrm{d}\nu}{\exp[h\nu/kT] - 1} . \tag{87}$$

Introducing the Debye temperature

$$\Theta = \frac{h\nu_m}{k}$$

and the following relation connecting the Helmholtz free energy F to the internal energy U:

$$F = T\int U \,\mathrm{d}\left(\frac{1}{T}\right) ,$$

we find

$$p_D = \frac{U_D}{v} \frac{\mathrm{d}\ln\Theta}{\mathrm{d}\ln v} . \tag{88}$$

If we set

$$\gamma = -\frac{\mathrm{d}\ln\Theta}{\mathrm{d}\ln v} = -\frac{\mathrm{d}\ln\nu_m}{\mathrm{d}\ln v} ,$$

we see that we obtain the same expression for the thermal pressure on the basis of Debye theory and on the basis of the Grüneisen theory. The thermal pressure is related to the pressure at absolute zero p_0 and the measured pressure p by

$$p = p_0 + p_D .$$

p_D is given in explicit form by

$$p_D = \frac{9NkT\gamma\varrho}{M} \frac{1}{x^3} \int_0^x \frac{\xi^3 \mathrm{d}\xi}{e^\xi - 1} \tag{89}$$

with

$$x = \Theta/T ,$$

where ϱ is the density, N is Avogadro's number and M is the atomic weight. Accurate tables of the integral which appears in (89) can be found in LANDOLDT-BORNSTEIN [85] or in KNOPOFF [58]. From the knowledge of γ and Θ, by means of (89) it is possible to estimate p_D at any given temperature. Θ can be determined from a measurement of the specific heat at constant volume:

$$C_v = \left(\frac{\partial U}{\partial T}\right)_v = \frac{\partial}{\partial T} \frac{9N_0}{\nu_m^3} \int_0^{\nu_m} \frac{h\nu^3 \mathrm{d}\nu}{\exp\,[h\nu/kT] - 1} ,$$

or by means of

$$C_v = \frac{9N_0 k}{x^3} \int_0^x \frac{\xi^4 e^\xi \mathrm{d}\xi}{(e^\xi - 1)^2} . \tag{90}$$

Another manner to estimate the Debye temperature is to use the following relation of easy demonstration:

$$\nu_m^3 = \frac{9N\varrho}{4M} \left(\frac{1}{V_P^3} + \frac{2}{V_S^3}\right)^{-1} , \tag{91}$$

where V_P and V_S are infinite medium velocities of compressional motion and shear waves respectively. The estimate of Θ based on (91) differs somewhat from that based on (90). This is very likely due to the fact that the usual measurements of the elastic-wave velocities are made at frequencies less than ν_m.

10. – Equation of melting.

An equation of melting was first developed by LINDEMANN [86] on the basis of classical physics. Actually when the temperature T_m at which the melting point occurs satisfies the inequality

$$T_m \gg \Theta ,$$

the internal energy can be written in the classical form

$$E = 3kT_m . \tag{92}$$

Moreover the classical frequency of a harmonic oscillator is given by

$$\nu = \frac{1}{2\pi A} \left(\frac{E}{m}\right)^{\frac{1}{2}} , \tag{93}$$

where E and m are the total energy and the mass of the oscillator, A is the amplitude of the oscillator. LINDEMANN assumed that, at melting, the collisions between neighbouring atoms induce a break-up of the crystal structure when the value of A approaches the lattice dimensions. Since A is proprortional to $v^{\frac{1}{3}}$, where v is the volume per atom, expressing E of (93) by (92), we obtain

$$\nu = \text{const} \cdot \left(\frac{T_m}{m}\right)^{\frac{1}{2}} \frac{1}{v^{\frac{1}{3}}} . \tag{94}$$

The frequency obtained by the Lindemann equation and the maximum frequency of oscillation calculated by Debye specific-heat equation are in excellent agreement, at least for metals [87].

In order to fit observed melting-point data for some materials, SIMON [88-90] has given the following empirical equation for the melting point of solids:

$$p_m + p_0 = a T_m^b , \tag{95}$$

where p_0 is the pressure at absolute zero and b, c are constants.

It is possible to derive (95) assuming that the Lindemann law and the Grüneisen equation of state hold. If $T_m \gg \Theta$, it is possible to replace the thermal energy U_D by the Boltzmann energy $3NkT_m\gamma$, obtaining

$$p_m - p_0 = \frac{3NkT_m\gamma}{v_m} , \tag{96}$$

where N is the number of atoms in the volume at the melting v_m. Since γ is constant,

$$\nu_m = \text{const} \cdot (v_m)^{-\gamma} .$$

The Lindemann law gives for the maximum frequency

$$\nu_m = \text{const} \cdot \left(\frac{T_m}{m}\right)^{\frac{1}{2}} \frac{1}{v_m^{\frac{1}{3}}} ; \tag{97}$$

substituting (97) in (96), we have

$$p_m - p_0 = \text{const} \cdot \frac{T_m^{6\gamma+1}}{6\gamma - 2} . \tag{98}$$

From (98) it is possible to obtain the Grüneisen ratio. Assuming that p_0 and $(6\gamma + 1)/(6\gamma - 2)$ are slowly varying functions of the thermodynamic variables, we obtain

$$\frac{\mathrm{d}^2 p_m}{\mathrm{d}T_m^2} = \text{const} \cdot \frac{3(6\gamma + 1)}{(6\gamma - 2)^2} T_m^{((6\gamma+1)/(6\gamma-2))-2} , \tag{99}$$

and from (98) and (99)

$$\gamma = \frac{1}{2} \frac{\mathrm{d}p_m/\mathrm{d}T_m}{T_m \, \mathrm{d}^2 p_m/\mathrm{d}T_m^2} + \frac{1}{3}. \tag{100}$$

This formula is not restricted to application at zero pressure. Since Grüneisen's ratio is dependent upon the volume, it will not be constant over a melting curve and will therefore, in general, differ from the value at zero pressure. The above formula allows one to compute Grüneisen's ratio at any temperature and pressure along the melting curve; the only assumption that is present in the derivation of this expression is that Grüneisen's ratio is a slowly varying function of temperature and pressure.

11. – Compression of solids by strong shock waves.

Detonation waves in which the pressure is of the order of some 10^{11} are common to modern high-explosive experimentation. When such a detonation wave interacts with an explosive-solid interface, a shock wave is transmitted into the solid. It is also possible to obtain pressures greater than 10^{12} by some modification of the simple in-contact explosive-solid geometry mentioned above. The problem is to derive from the experimental data so obtained the pressure-compression (density) relation. For such a purpose we shall derive the hydrodynamic relation and discuss the thermodynamic interpretation of experimental data. Generally in this interpretation two assumptions are made:

a) the measured p, v, E states are states of thermodynamic equilibrium;

b) the compression, for a given presure, is the same as that which would be produced by a hydrostatic pressure of the same magnitude.

The condition *a*) is satisfied if thermodynamic equilibrium is attained in 10^{-7} s or less [91]. The condition *b*) is probably not exactly fulfilled since the shock-wave compressions are one-dimensional. However the shock-wave results, in most cases, connect smoothly with the hydrostatic Bridgman's results at lower pressures.

To derive the hydrodynamic relations useful in the treatment of the shock-wave phenomena, let us consider a continuous flow. Then, indicating the density and mass velocity by ϱ and u respectively, time and space by t and x, in one-dimensional flow the relation

$$\frac{\partial \varrho}{\partial t} + u \frac{\partial \varrho}{\partial x} + \varrho \frac{\partial u}{\partial x} = 0 \tag{101}$$

expresses the fact that the time rate of increase of mass, in an element of volume $\mathrm{d}x$ and unit cross-section, must equal the net flux.

Since the material in consideration is treated as a perfect fluid, the forces on an element of mass are those arising from the pressure gradient and possible body forces, such as gravity. In the present considerations the latter is negligible so that a net force

$$\frac{\partial p}{\partial x}\,\mathrm{d}x\ ,$$

causes the mass $\varrho\,\mathrm{d}x$ to experience an acceleration, so that, by the second law of dynamics, we can write

$$\varrho\,\frac{\partial u}{\partial t} + \varrho u\,\frac{\partial u}{\partial x} = p\ , \tag{102}$$

where p is the pressure. Assuming no energy transport between mass elements, the entropy S_0 of each mass element remains constant and the same for all the elements. Then specific internal energy and pressure are given by the following adiabatic relations:

$$\mathrm{d}E = -p\,\mathrm{d}v = -f(\varrho, S_0)\,\mathrm{d}v\ , \tag{103}$$

where v is the specific volume. Let us, now, consider a semi-infinite ($x > 0$) homogeneous mass (pressure p_0, density ϱ_0 and zero particle velocity) for which the surface ($x = 0$) pressure is reduced to some lower value p_1. Let us assume that the surface pressure may be relieved either istantaneously or continuously. The former case may be associated with some interface effects in one-dimensional flow. The latter may be achieved by a piston accelerating in the $-x$ direction.

We want to determine the flow arising from the pressure release wave which propagates into the undisturbed material.

From (103) we have

$$\frac{\partial p}{\partial x} = \left(\frac{\partial p}{\partial \varrho}\right)_s \frac{\partial \varrho}{\partial x}; \tag{104}$$

substituting (104) into (102), dividing by the « sound speed »

$$c(\varrho) \equiv \left(\frac{\partial p}{\partial \varrho}\right)_s \tag{105}$$

and adding and subtracting the final equation to (101), we get

$$\frac{\partial \varrho}{\partial t} + (u + c)\frac{\partial \varrho}{\partial x} + \frac{\varrho}{c}\left[\frac{\partial u}{\partial t} + (u + c)\frac{\partial u}{\partial x}\right] = 0 , \tag{106}$$

$$\frac{\partial \varrho}{\partial t} + (u - c)\frac{\partial \varrho}{\partial x} - \frac{\varrho}{c}\left[\frac{\partial u}{\partial t} + (u - c)\frac{\partial u}{\partial x}\right] = 0 . \tag{107}$$

Equation (106) implies

$$\mathrm{d}\varrho + \frac{\varrho}{c}\,\mathrm{d}u = 0 \qquad \text{along} \qquad \frac{\mathrm{d}x}{\mathrm{d}t} = u + c , \tag{108}$$

and equation (107) implies

$$\mathrm{d}\varrho - \frac{\varrho}{c}\,\mathrm{d}u = 0 \qquad \text{along} \qquad \frac{\mathrm{d}x}{\mathrm{d}t} = u - c . \tag{109}$$

Both differential equations in x, equations of sonic disturbances propagating in the $+x$ and $-x$ directions, have a class (C^+ and C^- respectively) of solutions. These solutions are called characteristics. Every characteristic in the (x, t)-plane must transform to either a point or a curve in the (u, ϱ)-plane. Along the leading C^+ characteristic, corresponding to the first sonic disturbance into the rest state, the material is described in the plane by the point $u = 0$, $\varrho = \varrho_0$ corresponding to the rest state. This characteristic is the straight line

$$\frac{\mathrm{d}x}{\mathrm{d}t} = c(\varrho_0) .$$

Since it corresponds to a wave initiating at $x = 0$, $t = 0$, it is intersected by all C^- characteristics which initiate at $t = 0$. Hence the boundary conditions $u = 0$, $\varrho = \varrho_0$ are the same for each C^- characteristic. Thus the second pair of characteristic equations may be integrated, along $\mathrm{d}x/\mathrm{d}t = u - c$, to give

$$u = \int_{\varrho_0}^{\varrho} \frac{c\,\mathrm{d}\varrho}{\varrho} . \tag{110}$$

Now any x, t point within the flow may be reached by a C^- characteristic initiating at $t = 0$. Hence (110) gives the mass velocity at any point, as a function only of the density at that point, since C depends only on ϱ. It follows that the value of the integral is independent of the x, t path along which the integration is performed. The image of each C^+ characteristic is a point in the (u, ϱ)-plane which lies on the curve defined by (110). Since u, ϱ and, hence, c are constants on each C^+ characteristic, it follows that the family of C^+ char-

acteristics are straight lines, as indicated in Fig. 15. Taking into account the equation of a C^+ characteristic and that u (eq. (110)) and c both decrease as density decreases for a normal equation of state, it is apparent that density

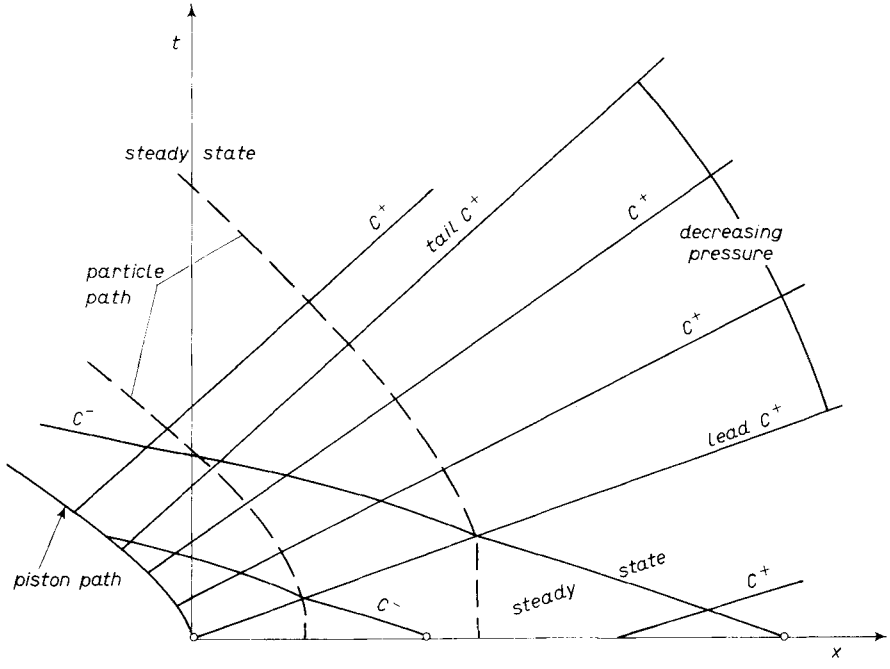

Fig. 15. – Distance-time plot of flow in a simple rarefaction wave.

or pressure decrease monotically with $\mathrm{d}x/\mathrm{d}t$, as indicated in Fig. 15. The tail C^+ characteristic, where the material attains the surface pressure p_1, is given by

$$\frac{\mathrm{d}x}{\mathrm{d}t} = \int_{\varrho_0}^{\varrho_1} \frac{c\,\mathrm{d}\varrho}{\varrho} + \left(\frac{\partial p}{\partial \varrho}\right)_{s,p=p_1} . \tag{111}$$

For this characteristic, $\mathrm{d}x/\mathrm{d}t$ is often positive; $\mathrm{d}x/\mathrm{d}t - u$, the velocity relative to the material, is always positive since

$$c = \left(\frac{\partial p}{\partial \varrho}\right)_s^{\frac{1}{2}} > 0 .$$

Summarizing, a mass point is undisturbed until its position is intersected by the leading C^+ characteristic. It then falls through the monotonically decreasing pressure gradient between the head and tail C^+ characteristics. Its velocity in this region is given by (110). The condition for monotonic behaviour, com-

bined with the condition $p = p_1$ on the material surface, requires that pressure, and hence the density and mass velocity, be uniform between the tail characteristic and the material surface. The velocity in this region is given by

$$u = \int_{\varrho_0}^{\varrho_1} \frac{c\,d\varrho}{\varrho} = \int_{p_0}^{p_1} \left(-\frac{\partial v}{\partial p}\right)_s^{\frac{1}{2}} dp \,. \tag{112}$$

The last integral in (112) is obtained from the first by use of (103) and (105) and the relation $\varrho = 1/v$.

Let us assume now that a piston moves into the semi-infinite mass in consideration, the velocity of the surface particles increasing with time. Since u increases along the piston path, the slopes $dx/dt = u + c$ increase along the piston path (see Fig. 16). The eventual crossing has the physically impossible

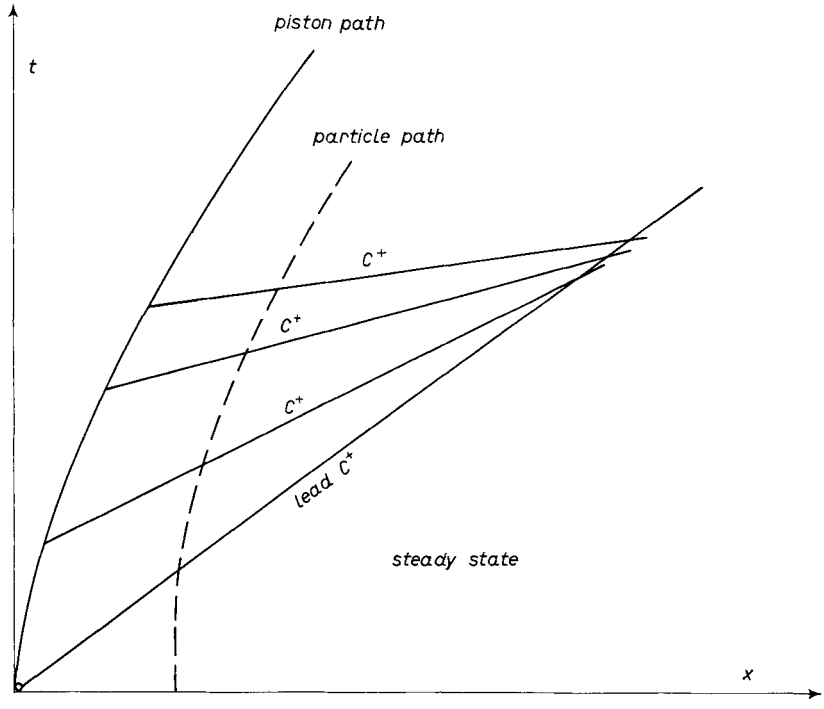

Fig. 16. – Distance-time plot of flow in a simple compression wave.

implication that more than one value of u and of ϱ is obtained for a given point in the (x, t)-plane. At times before the characteristics cross, the foregoing analysis yields a flow in which the pressure gradient increases with time. Actually the gradients increase until effects such as fluid viscosity, heat conduction, and

thermal nonequilibrium, all neglected above, play an important role in the flow. The ultimate pressure profile, which is time-dependent for fixed initial and final pressures, is called a shock front. In most applications, the shock front is sufficiently thin that it is convenient to regard it as a discontinuity. In the flow illustrated in Fig. 17, the disturbance corresponding to the shock front is propagated with a velocity u_s into an undisturbed state defined by pressure p_0, density ϱ_0 and mass velocity zero. The shock front is assumed to consist of a time-independent pressure profile. The pressure, density and mass velocity behind the front will be denoted by p_1, ϱ_1 and u_p, respectively. The relation

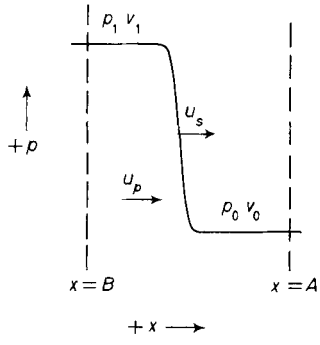

Fig. 17. – A shock front (p_1, v_1) is propagated with velocity u_s into an undisturbed state (p_0, v_0).

$$\varrho_0 u_s = \varrho_1(u_s - u_p) \tag{113}$$

expresses the condition that the mass flux in and out of the shock front must be equal. The net force on a unit cross-section of the material between $x = A$ and $x = B$ (see Fig. 17) is $p_1 - p_0$. The time rate of change of momentum for this material is the mass flux $\varrho_0 u_s$, through the shock multiplied by the associated velocity change u_p. Hence,

$$p_1 - p_0 = \varrho_0 u_s u_p \,. \tag{114}$$

The power input to a unit cross-section of material between A and B, $p_1 u_p$, must equal the time rate of change of energy for the enclosed material; that is,

$$p_1 u_p = \varrho_0 u_s \left(\frac{u_p^2}{2}\right) + \varrho_0 u_s (E_1 - E_0) \,. \tag{115}$$

Here E_0 and E_1 are the specific internal energies ahead of and behind the shock wave, respectively. Since, by combination of (113) and (114),

$$u_s = v_0 \sqrt{\frac{p_1 - p_0}{v_0 - v_1}} \tag{116}$$

and

$$u_p = \sqrt{(p_1 - p_0)(v_0 - v_1)} \,, \tag{117}$$

the velocities may be eliminated from the energy equation to give

$$E_1 - E_0 = \tfrac{1}{2}(p_1 + p_0)(v_0 - v_1) \,. \tag{118}$$

Equations (113), (114) and (118), expressing the conservation relations for a shock wave, were first derived by RANKINE and HUGONIOT. Since the specific internal energy of a material is a function of its pressure and volume, eq. (118) may be regarded as the locus of all p_1, v_1 states attainable by propagating a shock wave into a fixed initial state p_0, v_0. This locus is defined as the Hugoniot curve centred at p_0, v_0.

12. – Interpretation of shock-wave data.

We have already obtained the basic shock-wave equations relating the directly measured quantity u_p (particle velocity) and u_s (shock velocity) to the shock pressure p_H and energy per unit mass E_H:

$$u_s = v_0 \sqrt{\frac{p_H - p_{H0}}{v - v_0}}, \tag{116'}$$

$$u_p = \sqrt{(p_H - p_0)(v_0 - v)}, \tag{117'}$$

$$E_H = E_{H0} + \tfrac{1}{2}(p_H + p_{H0})(v_0 - v), \tag{118'}$$

where v_0 and v denote the specific volume of the sample before and during the shock. E_0, v_0 and p_0 are the quantities corresponding to the state before the passage of the shock front and may be taken at room conditions. Equations (116'), (117'), (118') allow us to determine the pressure and energy in the shocked material as a function of the volume. However, in almost all cases, u_s and u_p are related linearly:

$$u_s = C_0 + \lambda u_p, \tag{119}$$

where C_0 and λ are characteristics of the material considered. Equations (116'), (117') and (118) lead directly to a two-parameter equation for the Hugoniot curve:

$$p_H = p_{H0} + \frac{C_0^2(v_0 - v)}{[v_0 - \lambda(v_0 - v)]^2}. \tag{120}$$

To remove the temperature effect, *i.e.* to obtain the 0 °K isothermal equation of state, TAKEUCKI and KANAMORI [92] introduce Grüneisen's equation of state

$$p_H - p_K = \frac{\gamma}{v}(E_H - E_K), \tag{121}$$

where γ is Grüneisen's ratio and p_K is the pressure necessary for compres-

sing, at 0 °K, a material to a state having the same specific volume v as that under shock compression. E_K is the internal energy for the 0 °K isothermal compression and is related to p_K by

$$p_K = -\left(\frac{\partial E_K}{\partial v}\right)_T . \tag{122}$$

Equations (118′) and (121) lead to

$$\gamma = \frac{v(p_H - p_K)}{\frac{1}{2}(p_H + p_{H0})(v_0 - v) + E_{H0} - E_K} . \tag{123}$$

The volume dependence of γ is given by the Slater relation

$$\gamma = -\frac{v}{2}\frac{\partial^2 p/\partial v^2}{\partial p/\partial v} - \frac{2}{3} \tag{124}$$

or by the Dugdale-Mac Donald relation

$$\gamma = -\frac{v}{2}\frac{\partial^2 (pv^{\frac{2}{3}})/\partial v^2}{\partial (pv^{\frac{2}{3}})/\partial v} - \frac{1}{3} . \tag{125}$$

Equations (122), (123) and (124) or (125) are the basic equations determining the 0 °K isothermal p-v relation of the material.

Another method of reduction of the shock-wave equations of state to isothermal equations of state has been recently presented by SHAPIRO and KNOPOFF [83]. It is similar to that of TAKEUCHI and KANAMORI, but it is mathematically simpler and more readily adapted to numerical calculations. Moreover, unlike other treatments of shock-wave data, no extrapolations to zero temperature is required.

SHAPIRO and KNOPOFF [83] reduce the adiabatic quantities to isothermal ones, remarking that, although the Hugoniot equation is the sum of an elastic or zero-temperature energy and the thermal contribution, the Hugoniot pressure can be considered as the sum of the elastic pressure and a term proportional to the thermal energy density; the proportionality constant is γ. Thus,

$$E_H - E_{H0} = (E_c - E_{c0}) + (E_T - E_{T0}) = -\int_{v_0}^{v} p_c(v)\,\mathrm{d}v + \left[\frac{3RT}{M} f\left(\frac{\Theta(v)}{T}\right)\right]_{\substack{T=300^\circ \\ v=v_0}}^{v,T} , \tag{126}$$

$$p_H = p_c + p_T = p_c(v) + \frac{\gamma(v)}{v}\frac{3RT}{M} f\left(\frac{\Theta(v)}{T}\right) . \tag{127}$$

Here c and T denote cold and thermal quantities, R is the gas constant and f

is the Debye function. Equations (126) and (127) are derived on the assumption that the usual theory of atomic lattice vibrations applies, and terms giving the contributions of electrons to the energies have been neglected. However SHAPIRO and KNOPOFF give also the corrections for electronic pressures and energies. Moreover the volume dependence is given by

$$\gamma = \left(-\frac{\partial \ln H(v)}{\partial \ln v}\right)_T \tag{128}$$

and [78]

$$\frac{\Theta(v)}{\Theta_0} = \left[\frac{K_c(v)}{K_{c0}}\right]^{\frac{1}{2}} \cdot \left(\frac{v}{v_0}\right)^{\frac{1}{6}}, \tag{129}$$

where K_c is the isothermal pulse modulus, K_{c0} is the bulk modulus contribution from the nonthermal part only.

This method had been tested using the shock data of BAKANOVA *et al.* [93] for lithium. Columns 2 and 3 of Table VIII compare the theoretical results with those of BAKANOVA *et al.* The discrepancies arise from two sources. First, the Russian authors prefer Dugdale-Mac Donald formulation for γ, which generally gives smaller values of γ and therefore larger values for p_c. A more

TABLE VIII. – *Comparison of the theoretical results of* SHAPIRO *and* KNOPOFF *with experimental values of* BAKANOVA *et al.* (*from* [83]).

	$p_c \cdot 10^9$		
v_0/v	BAKANOVA *et al.*	SLATER	DUGDALE-MACDONALD
1.0	—3.18	—2.91	—2.91
1.1	9.65	8.32	8.67
1.2	24.5	20.8	22.0
1.3	41.3	35.0	37.2
1.4	59.9	51.5	54.7
1.5	80.3	70.4	74.4
1.6	102.4	91.9	96.5
1.7	126.1	115.7	120.8
1.8	151.4	141.5	147.3
1.9	178.3	169.3	175.8
2.0	206.6	198.7	206.3
2.1	236.4	229.8	238.5
2.2	272.3	262.2	272.4
2.3	300.2	296.0	307.9
2.4	334.1	331.1	345.0
2.5	361.9	367.3	383.4
2.6	406.0	404.5	423.3
2.7	443.9	442.8	464.5

important point is, however, that the earlier solution represents a parametric fit with the parameter chosen in such a way that a functional form for γ is selected which guarantees a best fit to the experimental Hugoniot curve. The justification for the use of such a method can lie only in its simplicity.

The procedure of SHAPIRO and KNOPOFF is modified only slighly if the Dugdale-Mac Donald formula is used instead of the Slater formula. Column 3 of Table VIII shows the results for lithium using Dugdale-MacDonald formula. However a significant disagreement with the solution of BAKANOVA *et al.* remains. The method here described can also be used for materials for which (129) does not hold.

13. – Relation of Thomas-Fermi equations of state to shock-wave measurements.

ALTSHULER *et al.* [6] have measured the compressibility of several metals to a pressure of the order of $4 \cdot 10^{12}$ using the technique of shock waves. In order to make a proper interpretation, the equation of state so determined was reduced to a reference temperature by KNOPOFF and MAC DONALD [7], using [6]

$$(130) \qquad p_c = -\frac{1}{2}\gamma^2(\varrho/\varrho_0)^{\gamma+1}\int_1^{\varrho/\varrho_0} p_h(x)(x-h)x^{-(\gamma+2)}\,\mathrm{d}x - \frac{1}{2}\gamma(\varrho/\varrho_0 - h)p_h(\varrho/\varrho_0)\,,$$

where p_c is the pressure at absolute zero, ϱ_0 is the density at zero pressure, $h = 2/\gamma + 1$, and γ is taken to be constant over the pressure range of interest. The reduction of the data depends very critically upon the value of γ. The Grüneisen ratio has been measured only for iron obtaining a value about 1.6 a pressure of 10^{12}.

KNOPOFF and MAC DONALD have computed the value of γ for the materials, for which no experimental measurement exists, on the basis of the Thomas-Fermi equation of state. The results obtained have been corrected using the experimental determination of γ for iron. The

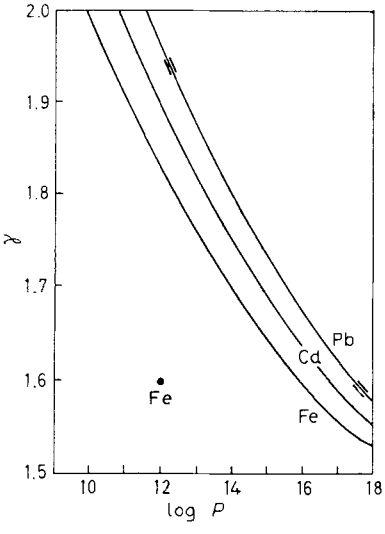

Fig. 18. – The variation of Grüneisen's ratio as a function of pressure for the Thomas-Fermi model of lead, cadmium and iron. The experimental determination by ALTSHULER *et al.* is shown as a point. (From [7].)

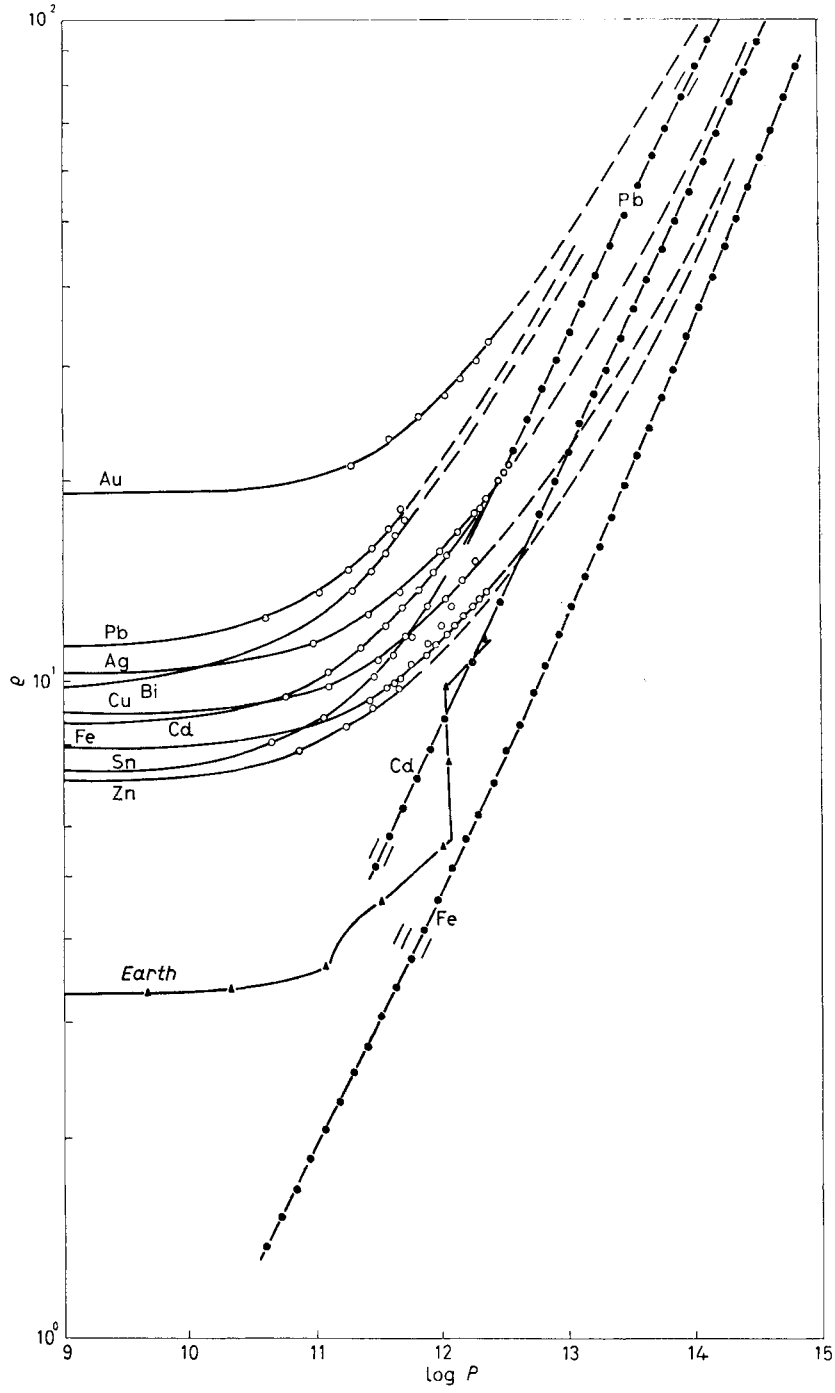

Fig. 19. – Experimentally determined equation of state of nine elements (open circles) reduced to absolute zero, compared with the Thomas-Fermi equation of state at absolute zero (full circles) and the equation of state for the Earth in Bullen's model (triangles). Extrapolation of the experimental data (dashes) is obtained by integration of the velocity equation of state. (From [7].)

quantum-mechanical calculation for γ yields values, in the pressure range where the quantum-mechanical model becomes significant, of the order of the values of γ determined experimentally at low pressures (Fig. 18).

The values of γ used fall in the range 1.3 to 1.6. The experimental equations of state at absolute zero have been drawn as the lines with open circles in Fig. 19. In order to interpolate between the experimental data and their quantum-mechanical asymptotes KNOPOFF and MAC DONALD use a velocity equation of state relating to pressure in the fluid state of the metal. Velocities derived from the Thomas-Fermi model are then compared with those obtained from the reduced data of shock-wave measurements. From Fig. 20 one can see that the velocity equations of state determined from experimental velocity data approach the quantum-mechanical equations of state at pressures much lower than those at which the corresponding density equations of state approach their quantum-mechanical asymptotes. The velocity distribution in the Earth can also be compared with the experimental determinations of the velocities since the pressure range is similar (Fig. 22). In Fig. 22 an expansion of the region pertinent to the core has been made. The velocity distribution in the core is in excess of the experimental values of the velocity in iron at absolute zero and is roughly identical to the Thomas-Fermi values of the velocity in iron. The velocity of seismic waves in the core is about 0.4 km/s higher than the experimental values for metallic iron. If there are no corrections for temperature, it is very likely that the velocity in the core is more appropriate to the material having atomic number 23 than to iron. The density of the core results, from experimental velocity data and the density equation of state, less than

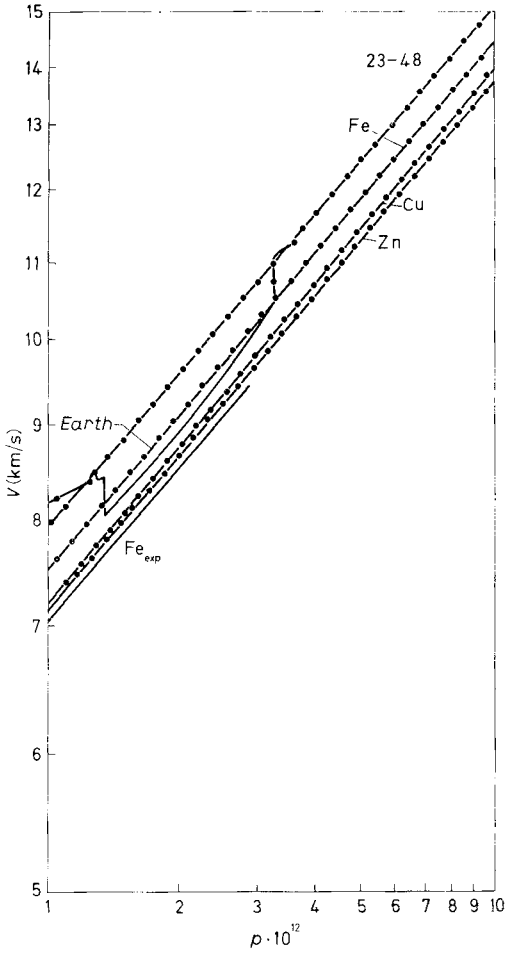

Fig. 20. – Velocity of sound in the fluid state at core pressures (from [7]).

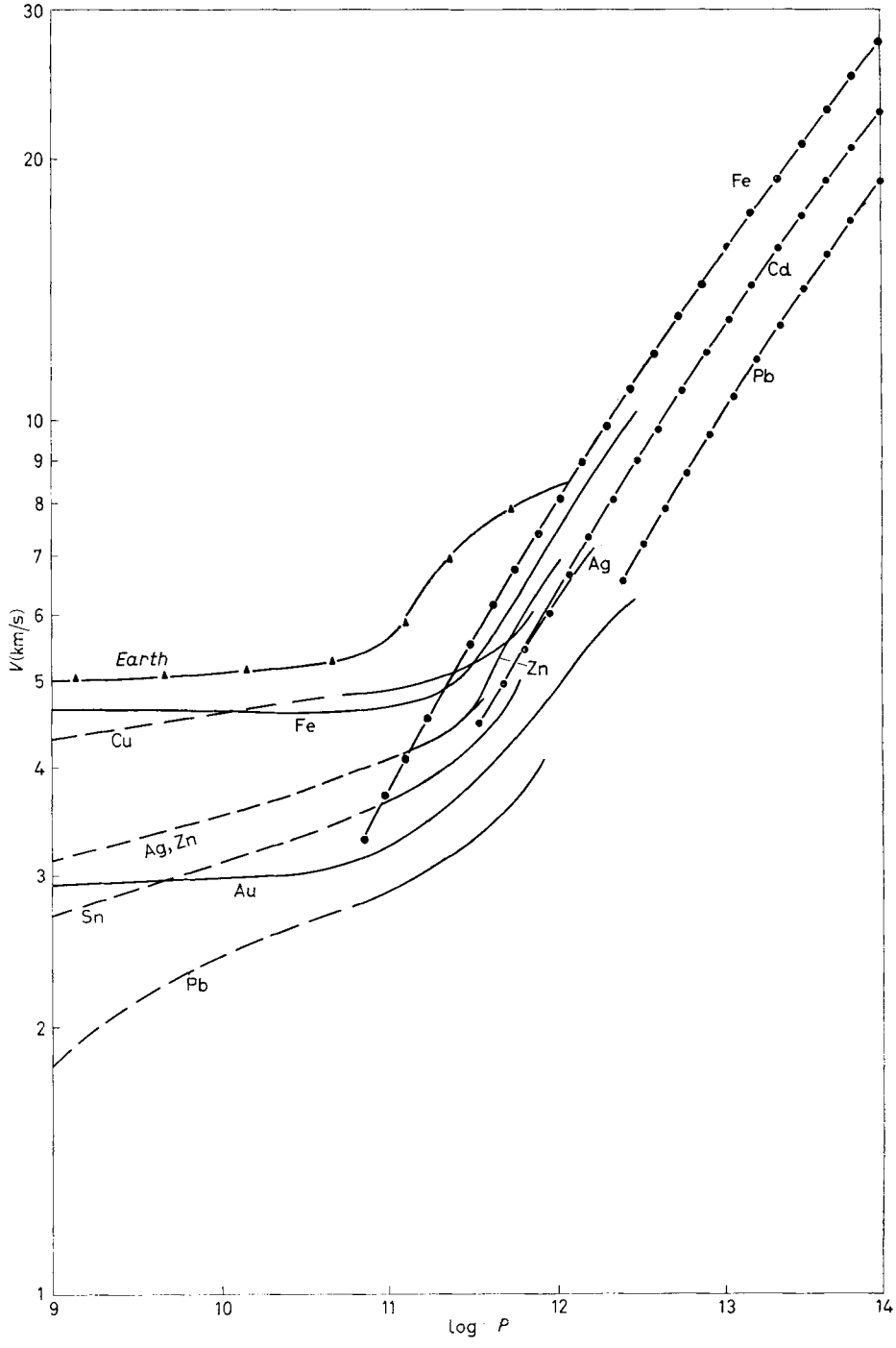

Fig. 21. – The variation with pressure of the velocity of sound in the fluid state. Velocities derived from the Thomas-Fermi model (full circles) are compared with those obtained from the reduced data of shock-wave measurements (solid curves). The seismic velocity distribution given by BULLEN (triangles) is also shown by comparison. The dashed curves represent the extrapolation to the zero-pressure value of $V = (\alpha^2 - \frac{1}{3}\beta^2)^{\frac{1}{2}}$. (From [7].)

that of iron. This can be seen in Fig. 21, where at absolute zero experimental equations of state of nine metals are compared with the density equation of state of the Earth. Without corrections iron density is of about 1.8 g/cm³ larger than that for the core. Also from these considerations the core must have an atomic number smaller than that for the iron if no corrections are applied (Fig. 20). KNOPOFF and MAC DONALD have shown that these differences can be reduced but still exist even when corrections are made to the experimental data to allow for the thermal expansion of iron to the temperatures of the core and for the volume change upon melting. The discrepancy can only be resolved if the core is not pure iron but contains significant amounts of elements of lower atomic number. Furthermore, any nickel alloyed with iron would increase the discrepancy since the density of pure nickel is 8.6 g/cm³ at room conditions, and the density of nickel is greater than that of iron at extremely high pressure.

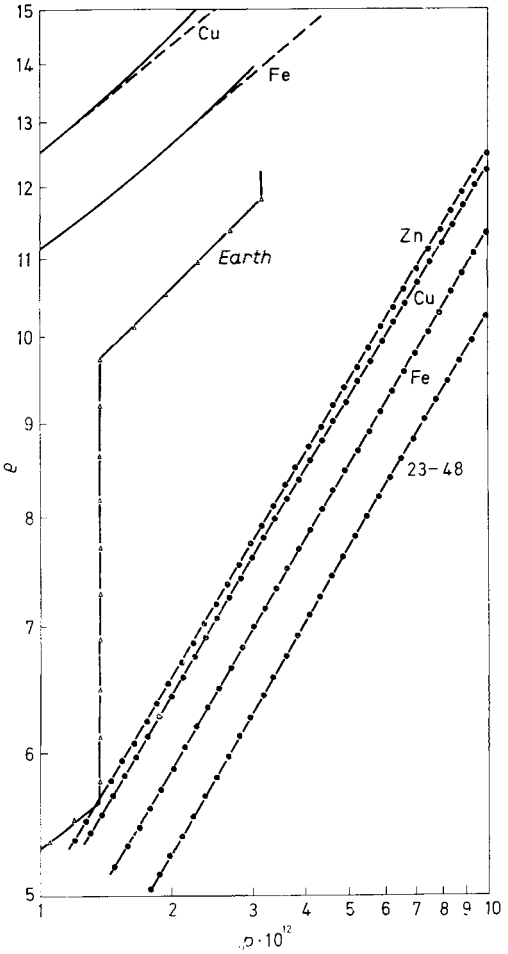

Fig. 22. – Equation of state for iron, copper, zinc and a hypothetical material of atomic number 23, atomic weight 48 in the core pressure range. The values derived from shock-wave measurements (solid) are compared with those obtained from the Thomas-Fermi theory (full circles). Bullen's density distribution is shown for comparison (triangles). (From [7].)

TAKEUCHI and KANAMORI [92] have numerically integrated their equations for Fe, Cu, Zn, Ag, Cd, Au and Pb using the experimental data of ALTSHULER *et al.* [6]. The equations of state at 0 °K so calculated are compared with the Murnaghan-Birch and Thomas-Fermi-Dirac equations of state. The Murnaghan-Birch equations of state are calculated for $\xi = -\frac{1}{2}, 0, \frac{1}{2}$. The Thomas-Fermi-Dirac data are those obtained by METROPOLIS and REITZ [94]. From Fig. 23-29 it can be seen that at lower pressures the Murnaghan-Birch curves with $\xi = 0$, $\approx -\frac{1}{2}$ fit the p-ϱ relations of all the metals except titanium,

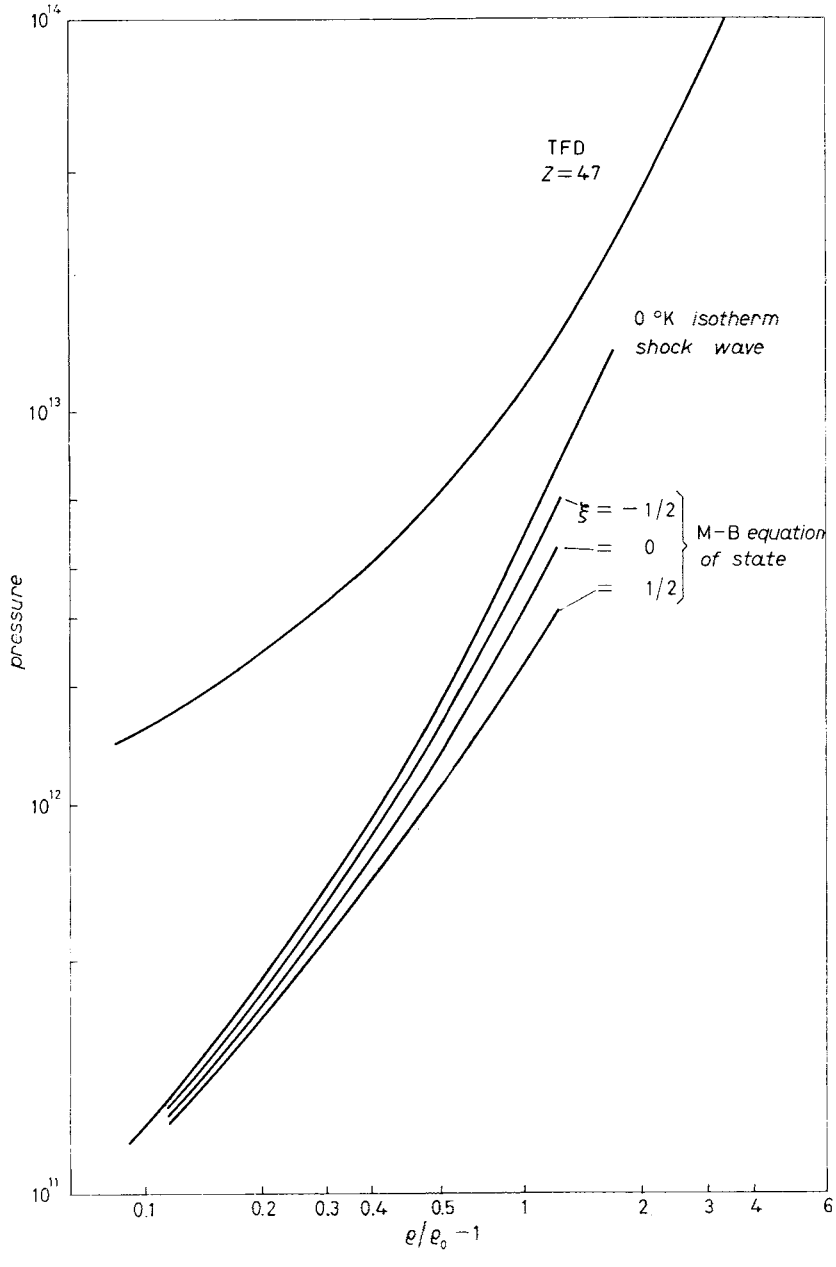

Fig. 23. – Isotherms of silver at 0 °K based on shock-wave data, Murnaghan-Birch model and Thomas-Fermi-Dirac model (from [92]).

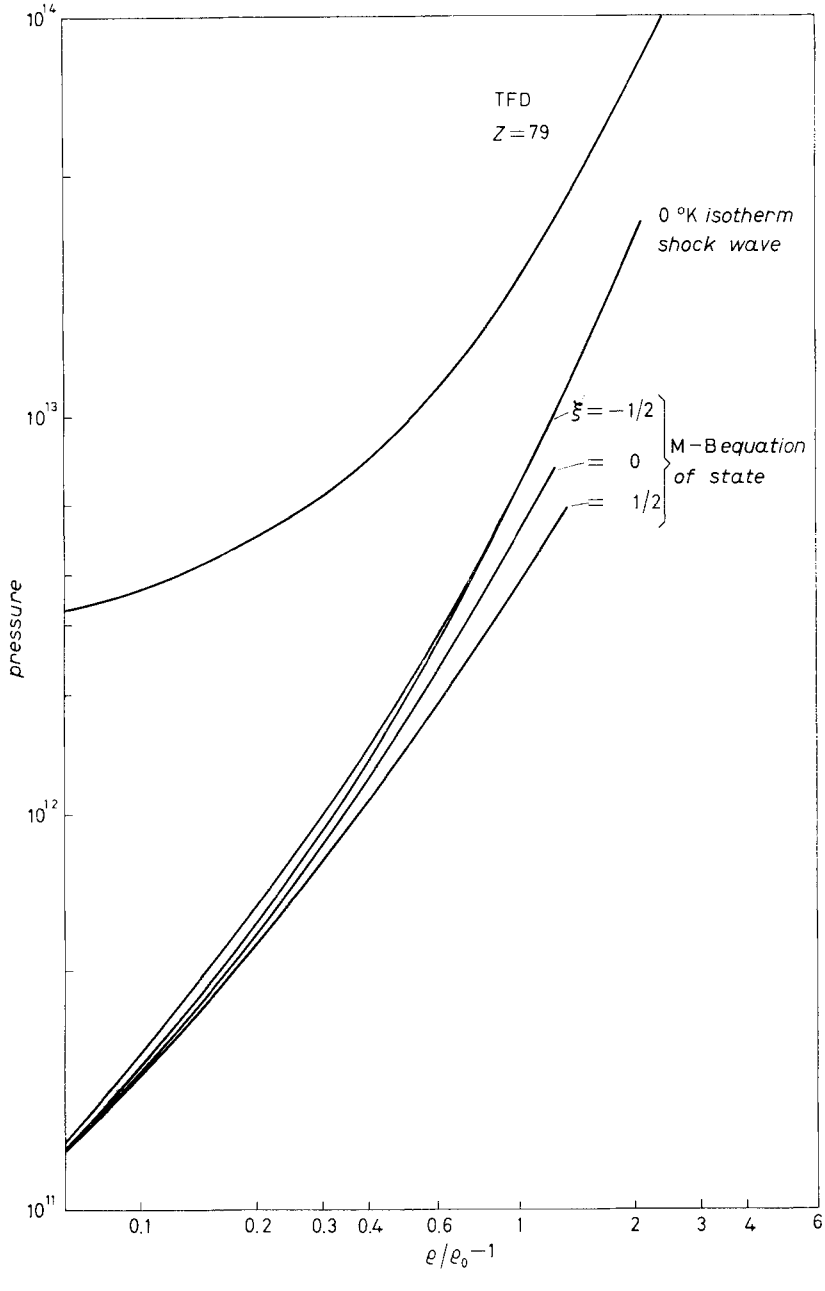

Fig. 24. – Isotherms of gold at 0 °K (from [92]).

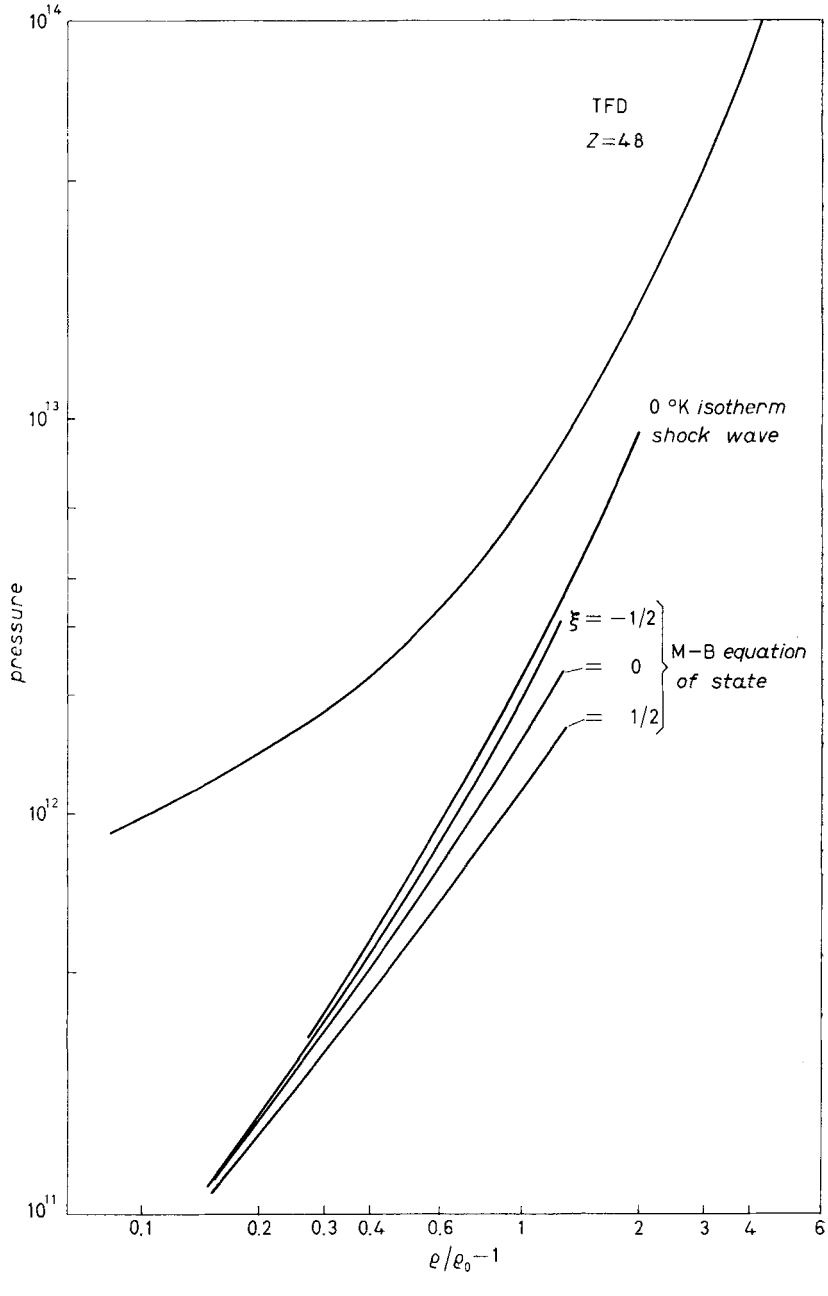

Fig. 25. – Isotherms of cadmium at 0 °K (from [92]).

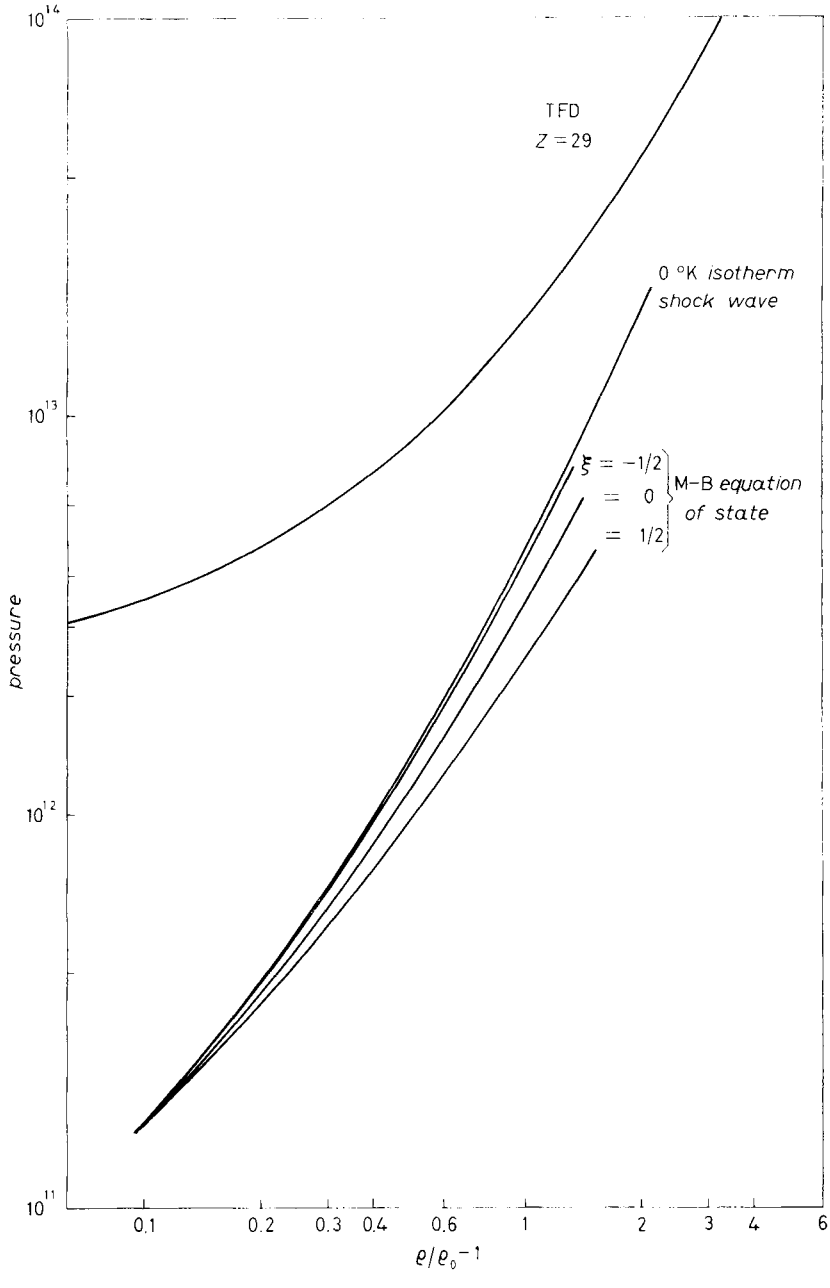

Fig. 26. – Isotherms of copper at 0 °K (from [92]).

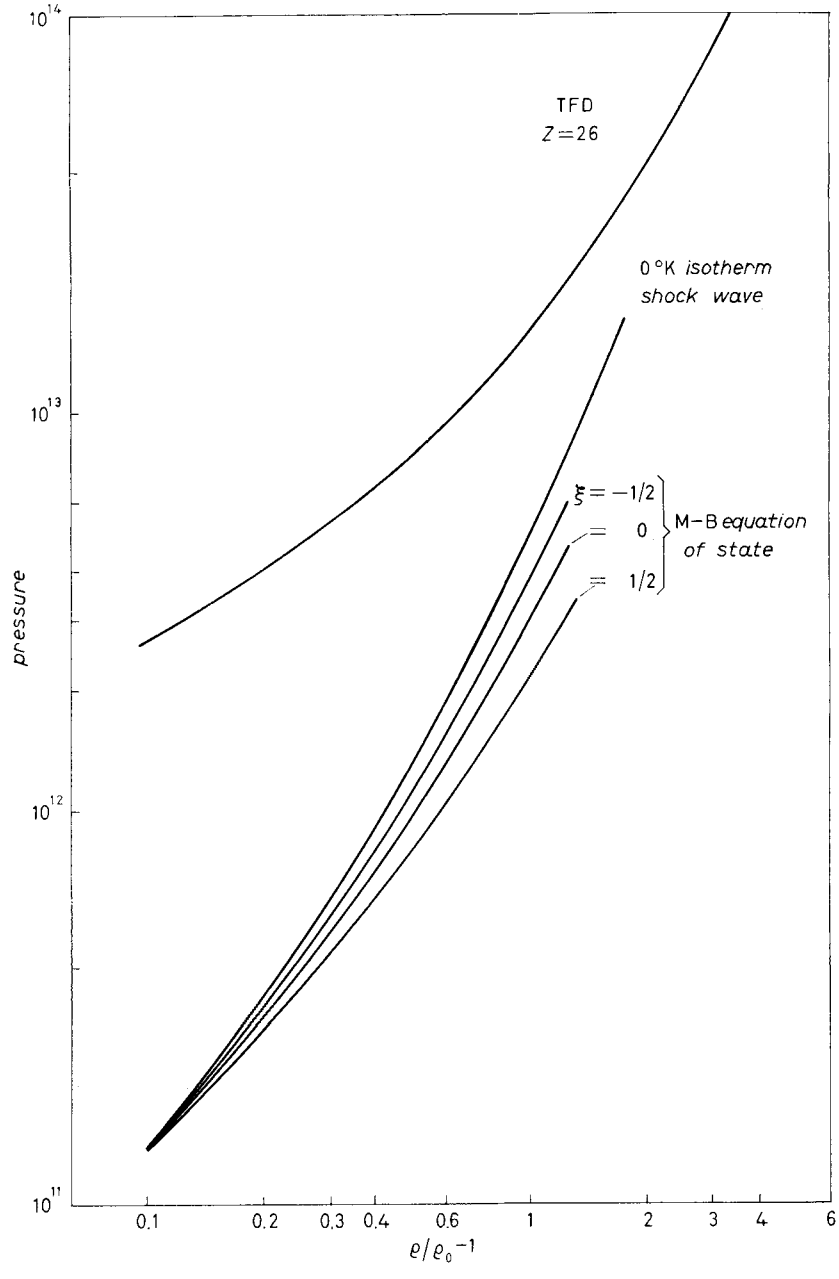

Fig. 27. – Isotherms of iron at 0 °K (from [92]).

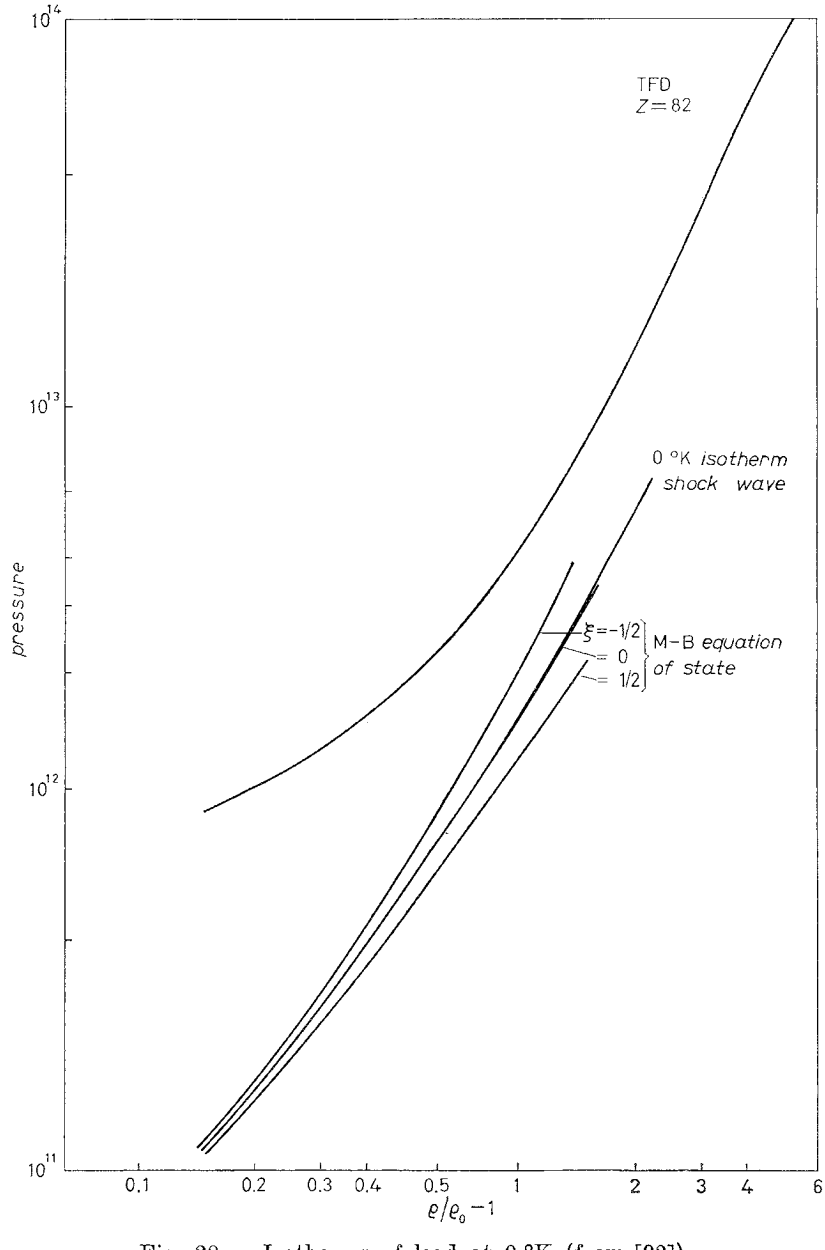

Fig. 28. – Isotherms of lead at 0 °K (from [92]).

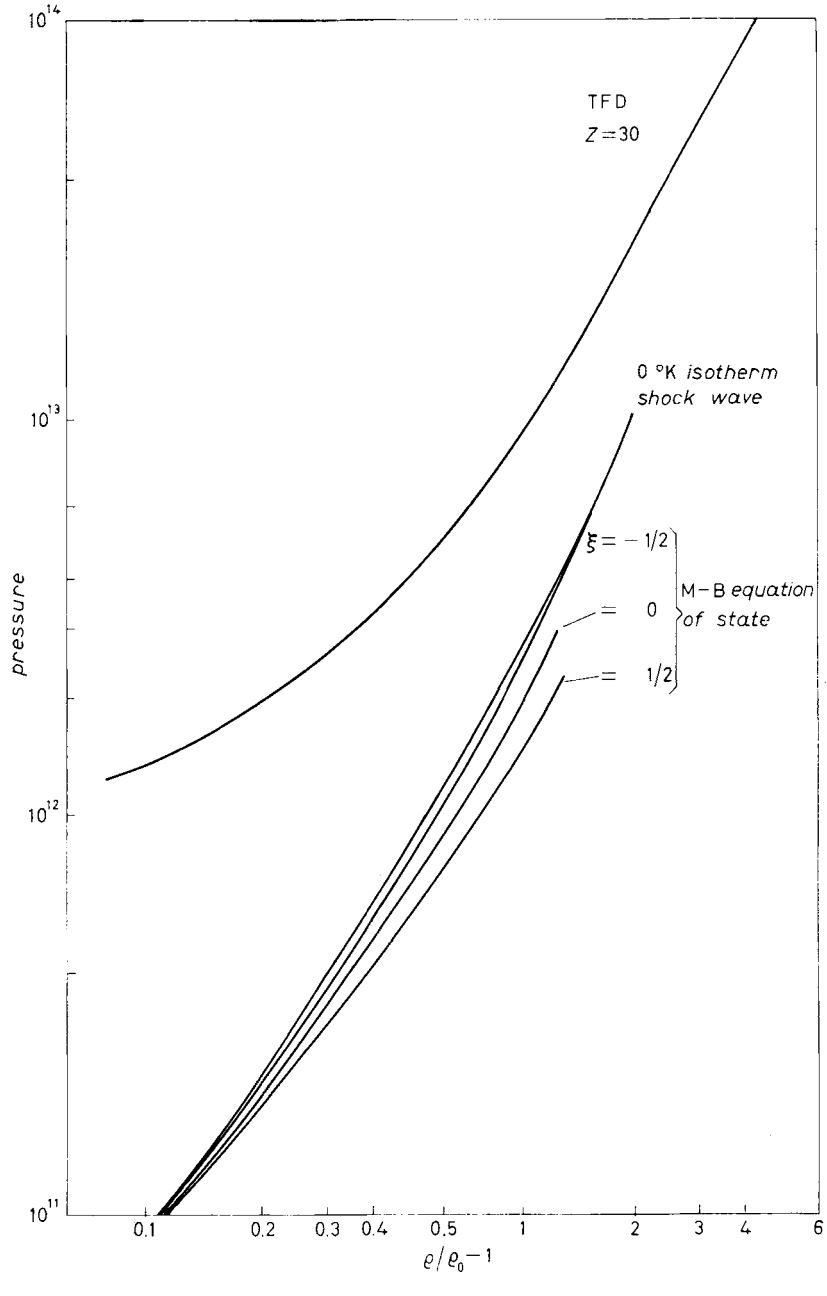

Fig. 29. – Isotherms of zinc at 0 °K (from [92]).

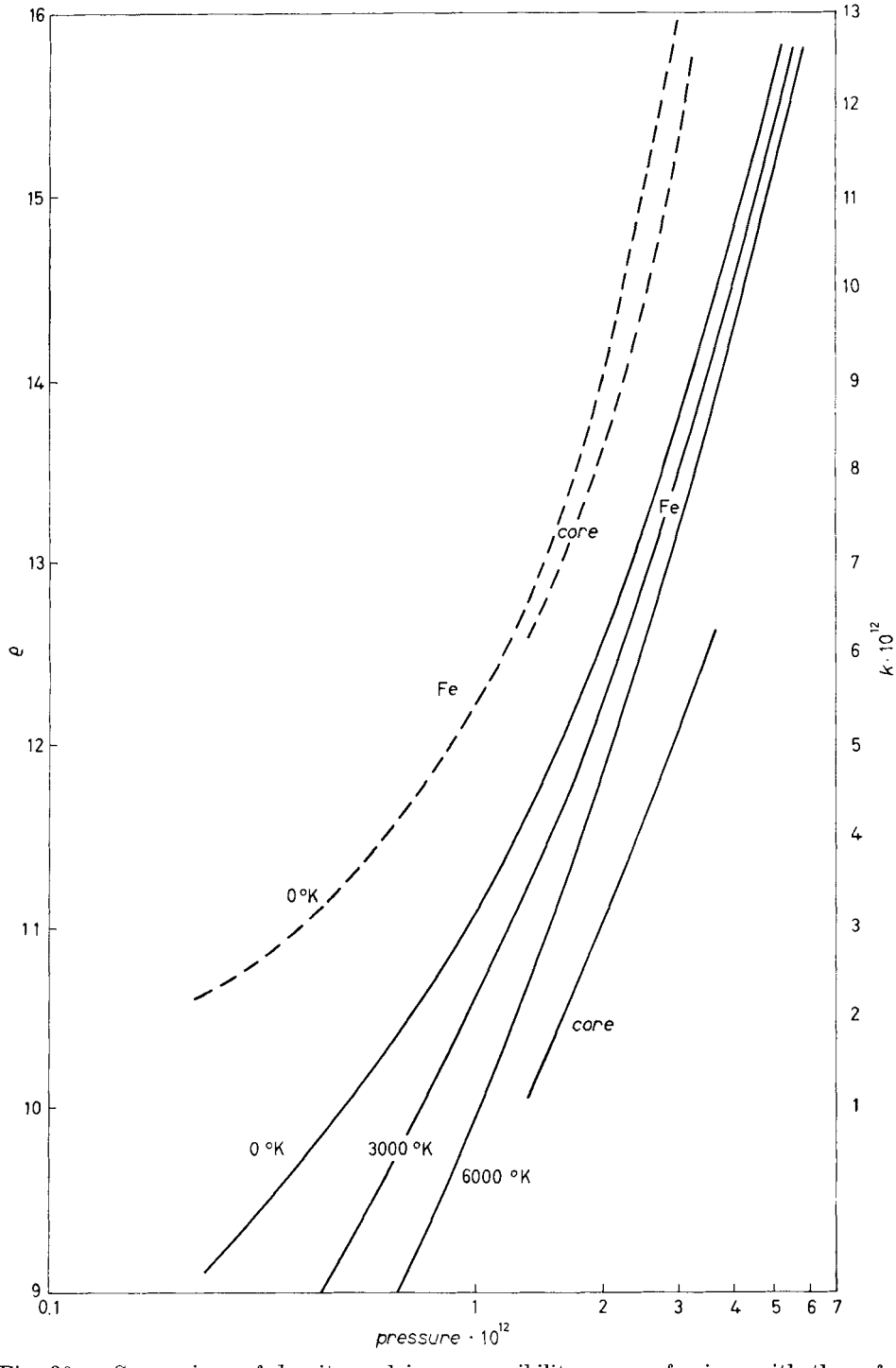

Fig. 30. – Comparison of density and incompressibility curves for iron with those for the Earth's core. Density distribution is based on Birch's solution I. (From [93].)
— — — K, ——— ϱ.

for which the p-ϱ curve is approximated by a Murnaghan-Birch curve with $\xi = \frac{1}{2}$. In other words, although the Murnaghan-Birch equation of state with $\xi = 0$ does not approximate the equations of state of all the metals studied as it does for a number of alkali metals [34], the equation of state having a small second-order coefficient ξ is quite appropriate for most of them. This second-order coefficient ξ may vary from one metal to another, and it can be said that the equation of state of a metal can essentially be determined by the two material constants, K_{H0} and ξ. For some metals, such as Ag, Cr and Fe, it can be seen that the 0 °K isotherm would deviate from the Murnaghan-Birch curve and merge into the Thomas-Fermi-Dirac curve at pressures a little higher than 10^{14}. In Fig. 30, the calculated density and incompressibility of iron are

TABLE IX. – *Incompressibilities of metals* ($\cdot 10^{12}$).

Metal	P_K		
	0	10^{12}	$4 \cdot 10^{12}$
ALTSHULER *et al.* [6]			
Ag	1.14	5.35	16.2
Au	1.92	6.69	16.8
Cd	0.61	4.36	13.9
Cu	1.36	5.35	15.5
Fe	1.14	5.52	16.8
Pb	0.60	3.65	10.9
Zn	0.73	4.44	13.8
McQUEEN and MARCH [95]			
Ag	1.10	5.47	16.8
Au	1.82	6.13	17.9
Cd	0.52	5.00	16.3
Co	1.99	5.65	14.8
Cr	1.93	6.14	16.6
Cu	1.39	5.60	16.1
Mo	2.71	6.14	14.6
Ni	1.91	5.98	16.3
Pb	0.47	4.29	13.9
Sn (gray)	0.51	4.21	13.4
Sn (white)	0.51	4.23	13.4
Th	0.53	3.55	10.7
Ti	1.03	3.62	9.51
Tl	0.41	4.21	13.7
V	1.59	4.77	12.4
W	3.07	6.64	15.6
Zn	0.66	4.76	15.2
$R = \frac{(2(K_{max} - K_{min})}{K_{max} + K_{min}}$	1.53	0.61	0.61

compared with those of the Earth's core. Three density curves are calculated for the temperatures of 0 °K, 3000 °K and 6000 °K. The temperature effect becomes small with increasing pressure. This Figure shows that the density of the Earth's core is 1 to 1.5 times smaller than that of iron at the pressure and temperature prevailing in the Earth's core. The incompressibility curve of iron at 0 °K is almost parallel to the incompressibility curve of the core. These results support the view of KNOPOFF and MAC DONALD. TAKEUCHI and KANAMORI have also tested the incompressibility-pressure hypothesis advanced by BULLEN [29]. In Table IX are listed the values of the incompressibility of the metals at 0 °K and at the pressures of 0, 10^{12}, $4 \cdot 10^{12}$. The range of variation of the values of incompressibility among the metals studied here can be expressed by

$$R = \frac{2(K_{\max} - K_{\min})}{K_{\max} + K_{\min}},$$

where $K_{\max}$ and $K_{\min}$ are the maximum and minimum values of of incompressibility. R decreases very rapidly from 1.53 to 0.61 when the pressure increases from 0 to 10^{12}. However, R does not change appreciably at pressures higher than 10^{12}. Consequently it is expected that the incompressibility might differ from one material to another by at least 60% even at $4 \cdot 10^{12}$, which is approximately the pressure at the Earth's centre. The incompressibility-pressure hypothesis might not be true in a strict sense, but one of the most important conclusion derived from the hypothesis, namely that a solid inner core accounts for the 10% increase in compressional wave velocity at the inner-core boundary, might still be valid for the following reason. If the inner core is not solid, its incompressibility should be about 20% larger than that of the outer core. Since incompressibility of the outer core is, as mentioned earlier, close to the incompressibility of iron, the incompressibility of the inner core should be about 20% larger than that of iron. As shown in Table IX it is rather difficult to find a metal that satisfies this requirement, and this could make it impossible for the inner core to be liquid.

From the analysis of the works published till now, it would seem interesting to extend to high pressures the experiments, so to reach those pressures for which the equations of state studied till now are valid. However, by modifying the assumptions on which the equation of state is based, *i.e.* the pressure distribution within the atom, we calculate that for atomic numbers of the order of 30, the lower limit of validity is lowered to some 10^{12}.

From this, the validity of at least one theoretical model is assured. Therefore it seems more interesting to improve our experimental knowledge by extending the temperature range at which the high pressure experiments are made. Also other considerations indicate that the experimental extension of the temperature range instead of the pressure range is recommended.

* * *

We wish to thank Profs. J. COULOMB and K. E. BULLEN for reading the manuscript and giving helpful suggestions.

REFERENCES

[1] H. JEFFREYS: *The Earth* (Cambridge, 1929).
[2] B. GUTENBERG: *Trans. Amer. Geophys. Un.*, **32**, 373 (1951).
[3] R. G. MACQUEEN, J. N. FRITZ and S. P. MARCH: *Journ. Geophys. Res.*, **69**, 2947 (1964).
[4] F. BIRCH: *Journ. Geophys. Res.*, **69**, 4377 (1964).
[5] F. BIRCH: *Geophysical applications of high pressure research*, in *Solids under Pressure*, edited by W. PAUL and M. D. WARSCHAUER (New York, 1963), p. 137.
[6] L. V. ALTSHULER, K. K. KRUPNIKOV, B. N. LEBEDEV, V. I. ZHUCHIKHIN and M. I. BRAZHNIK: *Žurn. Èksp. Teor. Fiz.*, **36**, 606 (1958); L. V. ALTSHULER, K. K. KRUPNIKOV and M. I. BRAZHNIK: *Žurn. Èksp. Teor. Fiz.*, **34**, 614 (1958).
[7] L. KNOPOFF and G. J. F. MACDONALD: *Geophys. Journ. Roy. Astron. Soc.*, **3**, 68 (1960).
[8] K. E. BULLEN: *Physics and Chemistry of the Earth*, vol. **1** (London, 1956), p. 68.
[9] L. V. ALTSHULER, S. B. KORMER, M. I. BRAZHNIK, L. A. VLADIMIROV, M. P. SPERANSKAYA and A. I. FUNTIKOV: *Sov. Phys. JETP*, **11**, 766 (1960).
[10] K. E. BULLEN: in *Mantles of the Earth and Terrestrial Planets*, edited by S. K. RUNCORN (London, 1967).
[11] R. A. W. HADDON and K. E. BULLEN: *Phys. of Earth and Planets*, **2**, 35 (1969).
[12] H. JENSEN: *Zeits. Phys.*, **111**, 373 (1938).
[13] W. KUHN and A. RITTMANN: *Geol. Rundschau*, **32**, 215 (1941).
[14] E. WIGNER and J. B. HUNTINGTON: *Journ. Chem. Phys.*, **3**, 764 (1935).
[15] R. KRONIG, J. DE BOER and J. KORRINGA: *Physica*, **12**, 245 (1946).
[16] W. H. RAMSEY: *Mon. Not. Roy. Astr. Soc. Geophys. Suppl.*, **5**, 409 (1949).
[17] W. M. ELSASSER: *Rev. Mod. Phys.*, **22**, 1 (1950).
[18] P. W. BRIDGMAN: *Proc. Am. Acad. Arts. Sci.* **76**, 1 (1945).
[19] P. W. BRIDGMAN: *Rev. Mod. Phys.*, **17**, 1 (1946).
[20] P. W. BRIDGMAN: *Proc. Am. Acad. Arts. Sci.* **76**, 55 (1948).
[21] W. H. RAMSEY: *Mon. Not. Roy. Astr. Soc.*, **108**, 406 (1948).
[22] W. H. RAMSEY: *Mon. Not. Roy. Astr. Soc. Geophys. Suppl.*, **6**, 42 (1950).
[23] K. E. BULLEN: *Nature*, **157**, 405 (1946).
[24] G. P. KUIPER: *The Atmospheres of the Earth and Planets* (Chicago, 1952).
[25] E. RABE: *Astrophys. Journ.*, **55**, 112 (1950).
[26] K. E. BULLEN: *Nature*, **211**, 396 (1966); *Mon. Not. Roy. Astr. Soc.*, **133**, 229 (1966).
[27] G. P. KUIPER: *Astrophys. Journ.*, **55**, 112 (1950).
[28] W. M. ELSASSER: *Science*, **113**, 105 (1951).
[29] K. E. BULLEN: *Mon. Not. Roy. Astr. Geophys. Suppl.*, **5**, 355 (1949).
[30] K. E. BULLEN: *Mon. Not. Roy. Astr. Geophys. Suppl.*, **6**, 50 (1950).
[31] E. C. BULLARD: *Verhandel. Ned. Geol. Mijnbouwk. Genootschap*, **18**, 23 (1957).

[32] K. E. BULLEN: *Mon. Not. Roy. Astr. Geophys. Suppl.*, **6**, 383 (1952).
[33] H. C. UREY: *The Planets, their Origin and Development* (New Haven, Conn., 1952).
[34] F. BIRCH: *Journ. Geophys. Res.*, **57**, 227 (1952).
[35] F. BIRCH: *Geophys. Journ.*, **4**, 295 (1961).
[36] L. KNOPOFF and R. J. UFFEN: *Journ. Geophys. Res.*, **59**, 471 (1954).
[37] F. WATSON: *Between the Planets* (Philadelphia, 1941).
[38] K. RANKAMA and T. SAHAMA: *Geochemistry* (Chicago, 1950).
[39] R. P. FEYMAN, N. METROPOLIS and E. TELLER: *Phys. Rev.*, **75**, 1561 (1949).
[40] P. GOMBÀS: *Die statistische Theorie des Atoms und ihre Anwendungen* (Vienna, 1949).
[41] E. TELLER: *Rev. Mod. Phys.*, **34**, 627 (1962).
[42] L. BRILLOUIN: *L'atome de Thomas-Fermi, Act. Sci. Industr.*, No. 160 (Paris, 1934).
[43] R. LATTER: *Phys. Rev.*, **99**, 510, 1854 (1955).
[44] P. A. KIRZHNITS: *Žurn. Èksp. Teor. Fiz.*, **5**, 64 (1957).
[45] S. G. BRUSH: *Progress in High-Temperature Physics and Chemistry*, vol. **1**, edited by C. A. ROUSE (New York, 1967).
[46] R. GROVER: *Journ. Math. Phys.*, **7**, 2178 (1966).
[47] A. A. DUFF: *Properties of Matter under Unusual Conditions*, edited by H. MARK and S. FERNBACH (New York, 1969).
[48] R. LATTER: *Journ. Chem. Phys.*, **24**, 280 (1956).
[49] J. C. SLATER and H. M. KRUTTER: *Phys. Rev.*, **47**, 559 (1935).
[50] J. J. GILVARRY: *Phys. Rev.*, **95**, 41 (1954); **99**, 550 (1954).
[51] N. H. MARCH: *Proc. Phys. Soc.*, A **68**, 726 (1955).
[52] N. H. MARCH: *Adv. Phys.*, **6**, 1 (1957).
[53] D. S. KOTHARY: *Mon. Not. Roy. Astron. Soc.*, **96**, 833 (1936); *Proc. Roy. Soc.*, A **165**, 486 (1938).
[54] G. KELLER and R. E. MEYEROTT: Argonne National Laboratory Reports 4771 and 4856 (1952).
[55] F. D. MURNAGHAN: *Amer. Journ. Math.*, **59**, 235 (1937).
[56] F. D. MURNAGHAN: *Finite Deformation of an Elastic Solid* (New York, 1951).
[57] F. BIRCH: *Phys. Rev.*, **71**, 809 (1947).
[58] L. KNOPOFF: *High-Pressure Physics and Chemistry*, vol. **1**, edited by BRADLEY (New York, 1963), p. 227, 247.
[59] F. D. MURNAGHAN: *Proc. Nat. Acad. Sci.*, **30**, 244 (1944).
[60] L. THOMSEN and O. L. ANDERSON: *Journ. Geophys. Res.*, **74**, 981 (1969).
[61] F. LONDON: *Trans. Far. Soc.*, **22**, 19 (1937).
[62] J. LENNARD JONES: *Handbuch der Physik*, Vol. **24**/2 (1933), p. 176.
[63] J. L. KAWANAN: *Journ. Chem. Phys.*, **12**, 467 (1944).
[64] K. T. LANGEMANN: *Journ. Chem. Phys.*, **14**, 743 (1946).
[65] L. PAULING: *Phys. Rev.*, **54**, 899 (1938).
[66] L. PAULING: *Journ. Amer. Chem. Soc.*, **69**, 542 (1947).
[67] E. WIGNER and F. SEITZ: *Phys. Rev.*, **46**, 509 (1934).
[68] P. GOMBÀS: *Zeits. Phys.*, **94**, 472 (1937); **95**, 687 (1937); **99**, 729 (1937); **100**, 599 (1937); **104**, 81, 592 (1937).
[69] P. GOMBÀS: *Zeits. Phys.*, **107**, 656 (1938).
[70] P. GOMBÀS: *Acta Phys. Hung.*, **1**, 301 (1952); *Ann. of Phys.*, **10**, 253 (1952).
[71] J. BARDEEN: *Journ. Chem. Phys.*, **6**, 372, 367 (1938).
[72] T. S. KUHN and J. H. VAN VLECK: *Phys. Rev.*, **79**, 382 (1949).
[73] F. SEITZ: *Modern Theory of Solids* (New York, London, 1940), p. 356, 384.
[74] G. MIE: *Ann. der Phys.*, **11**, 657 (1903).

[75] C. KITTEL: *Introduction to Solid-State Physics* (New York, 1956).
[76] J. G. SLATER: *Introduction to Chemical Physics* (New York, 1939).
[77] E. GRÜNEISEN: *Handbuch der Physik*, Vol. **10** (1926), p. 22.
[78] J. J. GILVARRY: *Phys. Rev.*, **102**, 308, 331 (1956).
[79] J. C. SLATER: *Phys. Rev.*, **57**, 744 (1940).
[80] T. S. DUGDALE and D. K. C. MACDONALD: *Phys. Rev.*, **89**, 832 (1953).
[81] T. H. K. BARRON: *Conference de physique des basses temperatures* (*Annex 1955-3, Suppl. Bull. Inst. Intern. du Froid*) (Paris, 1955), p. 448; *Phil. Mag.*, **46**, 720 (1955).
[82] T. H. K. BARRON: *Ann. of Phys.*, **1**, 77 (1957).
[83] J. N. SHAPIRO and L. KNOPOFF: *Journ. Geophys. Res.*, **74**, 1435 (1969).
[84] P. DEBYE: *Ann. der Phys.*, **39**, 784 (1912).
[85] LANDOLDT-BORNSTEIN: *Tables* (Berlin, 1961).
[86] F. A. LINDEMANN: *Phys. Zeits.*, **11**, 605 (1910).
[87] J. K. ROBERTS: *Heat and Thermodynamics* (Glasgow, 1940).
[88] F. SIMON: *Zeits. Elektrochem.*, **35**, 618 (1929).
[89] F. SIMON: *Trans. Far. Soc.*, **33**, 65 (1937).
[90] F. SIMON: *Nature*, **172**, 746 (1953).
[91] M. H. RICE, R. G. MCQUEEN and J. M. WALSH: *Solid-State Phys.*, **6**, 1 (1957).
[92] H. TAKEUCHI and H. KANAMORI: *Journ. Geophys. Res.*, **71**, 3985 (1966).
[93] A. A. BAKANOVA, I. P. DUDOLADOV and R. F. TRUNIN: *Sov. Phys. Solid State*, **7**, 1307 (1965).
[94] N. METROPOLIS and J. R. REITZ: *Journ. Chem. Phys.*, **19**, 555 (1951).
[95] R. G. MACQUEEN and N. H. MARCH: *Journ. Appl. Phys.*, **31**, 1253 (1960).

BIBLIOGRAPHY

L. C. R. ALFRED and N. H. MARCH: *Phil. Mag.*, **46**, 759 (1955).
L. C. R. ALFRED and N. H. MARCH: *Phys. Rev.*, **36**, 630 (1956).
R. A. BALLINGER and N. H. MARCH: *Proc. Phys. Soc.*, A **67**, 378 (1954).
K. E. BANYARD and N. H. MARCH: *Acta Cryst.*, **9**, 385 (1956).
K. E. BANYARD and N. H. MARCH: *Proc. Camb. Phil. Soc.*, **52**, 280 (1956).
J. BARDEEN and W. SHOCKLEY: *Phys. Rev.*, **80**, 72 (1950).
J. D. BERNAL: *Observatory*, **59**, 268 (1936).
B. A. BOLT: *Mon. Not. Roy. Astr. Soc. Geophys. Suppl.*, **7**, 360 (1957).
M. K. BRACHMAN: *Phys. Rev.*, **84**, 1263 (1951).
P. W. BRIDGMAN: *Phys. Rev.*, **60**, 351 (1941).
P. W. BRIDGMAN: *Proc. Am. Acad. Arts Sci.*, **77**, 187 (1949).
E. C. BULLARD and H. S. W. MASSEY: *Proc. Camb. Phil. Soc.*, **29**, 511 (1933).
K. E. BULLEN: *Introduction to the Theory of Seismology* (Cambridge, 1953).
K. E. BULLEN: *Seismology* (London, 1953).
K. E. BULLEN: *Ann. Geophys.*, **11**, 53 (1955).
K. E. BULLEN: *Nature*, **196**, 973 (1962).
P. P. DEBYE and E. M. CONWELL: *Phys. Rev.*, **93**, 693 (1954).
P. A. M. DIRAC: *Proc. Camb. Phil. Soc.*, **26**, 376 (1930).
A. EUCKEN: *Naturwiss.*, **32**, 112 (1944).

A. EUCKEN: *Naturwiss.*, **33**, 311 (1964).
E. FERMI: *Zeits. Phys.*, **48**, 73 (1928).
R. P. FEYNMAN: *Phys. Rev.*, **56**, 340 (1939).
J. J. GILVARRY and G. H. PEEBLES: *Phys. Rev.*, **99**, 550 (1955).
J. J. GILVARRY: *Journ. App. Phys.*, **28**, 1253 (1957).
J. J. GILVARRY: *Journ. Atmos. Terrest. Phys.*, **10**, 84 (1957).
P. GOMBÀS: *Zeits. Phys.*, **121**, 523 (1943).
P. GOMBÀS: *Acta Phys. Hung.*, **3**, 105 (1953).
P. GOMBÀS: *Acta Phys. Hung.*, **3**, 127 (1953).
P. GOMBÀS: *Ann. of Phys.*, **18**, 1 (1956).
H. JENSEN: *Zeits. Phys.*, **82**, 794 (1933).
H. JENSEN: *Zeits. Phys.*, **89**, 713 (1934).
H. JENSEN: *Zeits. Phys.*, **93**, 232 (1935).
J. H. D. JENSEN and J. M. LUTTINGER: *Phys. Rev.*, **86**, 907 (1952).
L. KNOPOFF: *Journ. Chem. Phys.*, **28**, 1067 (1958).
A. LATTER and R. LATTER: *Journ. Chem. Phys.*, **25**, 1016 (1956).
H. W. LEWIS: *Phys. Rev.*, **111**, 1554 (1958).
G. J. F. MACDONALD and L. KNOPOFF: *Geophys. Journ.*, **1**, 284 (1958).
J. MACDOUGALL and E. C. STONER: *Phil. Trans.*, A **237**, 67 (1938).
R. G. MACQUEEN and S. P. MARCH: *Journ. Geophys. Res.*, **71**, 1451 (1966).
R. G. MACQUEEN, S. P. MARCH and J. N. FRITZ: *Journ. Geophys. Res.*, **72**, 4999 (1967).
N. H. MARCH: *Acta Cryst.*, **5**, 187 (1952).
N. H. MARCH: *Proc. Camb. Phil. Soc.*, **48**, 665 (1952).
N. H. MARCH: *Phil. Mag.*, **44**, 1193 (1953).
N. H. MARCH: *Proc. Phys. Soc.*, A **67**, 9 (1954).
N. H. MARCH: *Symposium on Band Structures*, edited by R. R. E. MALVERN (1954), p. 24.
N. H. MARCH: *Physica*, **22**, 311 (1956).
N. H. MARCH and J. S. PLASKETT: *Proc. Roy. Soc.*, A **235**, 419 (1956).
R. E. MARSHAK and H. A. BETHE: *Astrophys. Journ.*, **91**, 239 (1940).
R. E. MARSHAK, P. N. MORSE and H. YORK: *Astrophys. Journ.*, **111**, 214 (1950).
W. H. RAMSEY: *Occ. Notes Roy. Astr. Soc.*, **3**, 87 (1954).
F. SEITZ: *Phys. Rev.*, **47**, 400 (1935).
J. G. SLATER: *Phys. Rev.*, **81**, 385 (1951).
A. SOMMERFIELD: *Zeits. Phys.*, **78**, 283 (1932).
A. SOMMERFIELD: *Nuovo Cimento*, **15**, 14 (1938).
E. C. STONER: *Phil. Mag.*, **28**, 257 (1939).
L. H. THOMAS: *Proc. Camb. Phil. Soc.*, **23**, 542 (1927).
L. H. THOMAS: *Journ. Chem. Phys.*, **22**, 1758 (1954).
E. WIGNER: *Phys. Rev.*, **43**, 804 (1933).
E. WIGNER: *Phys. Rev.*, **46**, 1002 (1934).